Accepted manuscript (author version)

To appear in:

Iranian Journal of Earth Sciences (Iran J. Earth. Sci.)

E-ISSN: 2228-785X Print ISSN: 2008-8779

Received: 15 April 2025

Revised: 27 July 2025

Accepted: 18 September 2025

DOI: https://doi.org/10.57647/ijes.2026.18283

Review Articles

Seismic Gap Analysis on Fault Rupture Zones Using MMI and PGA Data (M≥5, Tehran & Central Alborz)

Abolfazl BaliLashak[1], Arezou Dorostian[1], Mehdi Zare[2]*, Elham Bostan[3], Aref BaliLashak[4]

[1]Department of Geophysics, NT.C., Islamic Azad University, Tehran, Iran

[2]Interational Institute of Earthquake Engineering and Seismology (IIEES), Tehran, Iran

[3]Department of Geology, Ka.C., Islamic Azad University, Alborz, Iran

[4]Faculty of Electrical and Computer Engineering, Malek-Ashtar University of Technology, Tehran, Iran

* Corresponding author: mzare@iiees.ir

Abstract

The historical and instrumental seismic activity in Tehran and the southern Central Alborz indicates that this region is susceptible to a potential future earthquake. Based on this premise, the present study identifies seismic hazard zones associated with seismic gaps and outlines vulnerable areas that could be impacted by a future event. These areas are characterized by soft soils, deteriorating urban infrastructure, and high population density—conditions conducive to strain accumulation and release. Zones exhibiting seismic locking are considered potential sites for significant earthquakes. Although these areas have high seismic potential, major events may not occur for extended periods. However, by considering the length of the rupture zone and the seismic history of the fault, it is possible to estimate the magnitude, probable location, and recurrence interval of the next earthquake. To this end, spectral mapping within a Geographic Information System (GIS) framework was employed to classify the ruptured fault zone using seismic intensity data derived from the Modified Mercalli Intensity (MMI) scale, based on strong ground motion (PGA) records. This dataset served as a layer of information for identifying seismic gaps likely associated with future events. Considering the distribution of related earthquake events, the Modified Mercalli Intensity zones near the causative fault can be identified as the rupture zones potentially triggering a future earthquake, thereby determining seismic gaps in the Tehran

region.Based on thisanalysis, three zones, labeled "A,B and C" were identified. With The occurrence of an earthquake in southern Tehran validating zone "B".

Keywords: S-wave velocity (30 m), Seismic gap, Rupture zone, Modified Mercalli Intensity (MMI), Strong ground motion (PGA), Isoseismal zones

1. Introduction

Modeling sedimentary basins involves understanding the interrelationships between sediment characteristics and seismic responses. Factors such as structure, texture, and grain size contribute to enhanced seismic effects and increased damage during weak earthquakes. To assess these characteristics, microseismic studies and earthquake catalogs can be used to evaluatesite effects, identify bedrock, and evaluate site zones, which are influenced by earthquake events and the development of shear modulus due changes in paper explores resulting from seismic activity. This and the rationale nature of using seismic hazard analysis. Employing Information layers associated with analysis, employing information assessspatial hazard without making temporal prediction.The assess spatial includes gathering baseline information, predictions. The concepts, summaries, general data, tables, and informational layers. Mapping historical and instrumental earthquakes layers, as well as mapping study area from various Seismic sources.Determining the maximum expectedmagnitude;Calculating seismicity parameters identifyingseismic sourcemodels and zones related toseismic gaps for future events withprioritization; and calculatingstrong ground motion parameters.seismic hazard analysis is performedby developing intensity based on the Modified MercalliIntensity (MMI)Scale to identify areas linked toseismic gaps withinthe study area.The study investigates the seismic hazard level in Tehran, and then a microzonation is performed using the MMI scale. The validation is performed for a small magnitude event that recently happened in the region.

(Norouzi, 1978) proposed attenuation relationshipsfor PGA based on the moment magnitude scale (Mw); (GhodratiAmiri, 2007) for PGA and SA based on the surface wave magnitude scale (Ms); (Zaferani and Noorzad, 2013) for PGA and SA based on Mw. (GhodratiAmiri, 2007) for PGA and SA based on for PGA and SA based on Mw. (Zaferani and Noorzad, 2013) for PGA and SA based on Mw; each of which proposed attenuation relationships for two site conditions: rock and soil.These studies derivedthe attenuation relationships by considering thedistance, earthquake magnitude, thenatural period of soil layer, and its material compositionwhile omittingother

predictive variables such asfaulting mechanism due to lack of relevantdata.It is important tonote that the Modified Mercalli Intensity (MMI) scale is anintensity-based measureof seismic shaking that assesses the effects of an earthquake at a specific location (Xu and Wang, 2021). As such, it can be usedto prioritize seismic events.

2. Literature Review and Definitions

To predict PGA (Peak Ground Acceleration), PGV (Peak Ground Velocity), and PGD (Peak Ground Displacement) at a given site, three categories of information are required: (1) geological data of the study area and existing faults, (2) seismological data, including the magnitude of seismic events and their distance from the site (in this study, MMI is used to represent areas affected by seismic events originating from the rupture zone), and (3) geotechnical properties such as the type and depth of soil at the site (VS30 values, which overlap with the MMI zone and rupture zone extent) (Malhotra, 2021). According to the Road, Housing, and Urban Development Research Center, Iran's seismic building design code (Standard 2800) provides a seismic hazard zoning map for a 475-year return period but does not detail the methodological steps for estimating PGA (Zare, 2017).

Strong ground motion PGA represents the maximum ground acceleration that occurs at a location during an earthquake, essentially the peak absolute acceleration recorded on an accelerogram at a specific site during the event (Özener et al., 2018). Zare, through reviewing seismic hazard zoning studies in Iran from 1970 to 2015 and strong ground motion values, published the first strong ground motion zoning map for Tehran (Zare, 2017). The first national seismic hazard zoning map of Iran for design-level earthquakes (475-year return period) was published in 1999 as an annex to the seismic code (Standard 2800) by Berberian and colleagues (Zare et al., 1999; Berberian and yeats, 2001). Spectral zoning maps were created using region-specific ground motion prediction equations that incorporated parameters such as spectral acceleration, PGV, and PGA (Malhotra, 2021). The use of both deterministic and probabilistic strong ground motion values has always proven to be an effective method. By developing hazard zoning maps and utilizing historical data, magnitude assessments can be made. According to Zare, the development of hazard maps and realistic approaches will improve seismic hazard analysis in Iran (Hassankhani and Aram, 2017).

considering 20 seismic zones in Iran, have estimated the maximum horizontal acceleration PGA for return periods of 75 and 475 years (Tavakoli and Ghaforyashtiany, 1999).considering 25 potential earthquake Seismic sourcess, has presented the estimated values of PGA and spectral acceleration in a period of 0.2 seconds for return periods of 475 and 2475 years in the form of zoning maps (Ritz et al., 2012). Using the classification of the seismic effect of the site affected by the earthquake, it has been carried out to find the relationship between the structure of sedimentary basins and the intensity and variability of the damages caused by it. Studies have also been reported on the identification of the Seismic sourceseffect using the site effect (after noise removal) in seismic receipts and the difference between receipts at the time of the earthquake, using PGA strong ground motion records (Xu and Wang, 2021).Maghami showed that although for relatively shallow bedrock (80 to 100 m) the velocity differences obtained in deep sediments from microseismology are estimated to be less than 10 to 15%, empirical relationships can also be obtained to estimate the bedrock depth (Maghami et al., 2021).

The North Anatolian Fault Zone in the Sea of Marmara, which has not had a major event since 1766. Considering that it has an annual slip fraction of 20 mm according to GPS network data, changes in the fault length and areas likely to be seismically absent, the division of the fault into probable segments, the interaction between seismicity and background seismicity, and simultaneous slip between isolated segments, has been introduced as likely to cause a seismic event with a magnitude greater than 7.0 (Özener et al., 2018). This area has a high correspondence with the epicenter of the Turkish Hero Marash seismic event (2023).

Relationship of Mmax to the stabilized fault length and uncertainties:

The maximum expected magnitude (Mmax) is usually related to the stabilized fault length, because the fault length is a key factor in determining the amount of energy released during tectonic rupture. This relationship is usually determined through empirical relationships and statistical models such as the Wells and Coppersmith relationship (Coppersmith and Wells, 1994).Methods for determining Mmax based on fault length (Bommer and Verdon, 2024): Empirical models: Using data from past earthquakes to determine the relationship between fault length and earthquake magnitude, Statistical models: Analyzing seismic data and using statistical distributions such as the Gutenberg-Richter model to determine, Physical models: Examining the

mechanical properties of the fault, such as slip rate and accumulated stress, to determine the maximum possible magnitude

Uncertainties in Determining Mmax (RivasMedina and Benito, 2018): The determination of Mmax is associated with several uncertainties that can affect the accuracy of predictions. These include: uncertainty in historical data, as the lack of seismic records in some areas reduces the reliability of empirical models; uncertainty in tectonic properties, since variations in slip rate, fault depth, and geological conditions can influence Mmax; uncertainty in statistical models, because different models used to estimate Mmax may yield varying results; and uncertainty in stress distribution, as tectonic stresses along the fault may not be uniformly distributed, thereby affecting the earthquake magnitude.

Thus, Mmax is usually related to the established length of the fault, but tectonic, statistical, and historical data uncertainties can affect the accuracy of this prediction. To reduce these uncertainties, the use of hybrid models, extensive seismic data, and advanced statistical analyses is recommended.Integrating the spatial distribution map of Vs30 values with seismic hazard assessment in Alborz and Tehran to determine seismicity requires combining geophysical, tectonic, and seismic data. Vs30, which represents the shear wave velocity in the surface layers of the earth, plays an important role in modeling the seismic response of soil and seismic hazard zoning. Relationship of Vs30 to Seismic Hazard Assessment (Alikhanzadeh and Zafarani, 2023):Low Vs30 values indicate soft and sedimentary soils that can amplify seismic waves and increase seismic hazard, High Vs30 values are usually seen in rocky and stable areas that can reduce seismic effects. Areas with seismicity may have specific Vs30 values that indicate the absence of large seismic waves in the past.

Methods for Integrating Vs30 Maps with Seismic Absence Assessment (Alikhanzadeh and Zafarani, 2023): Correlation Analysis between Vs30 and Seismic Data: Investigating the relationship between Vs30 values and the region's seismicity rate to identify areas of seismic absence.

Seismic Hazard Modeling Using GIS: Integrating Vs30 Maps with Fault Data, Historical Earthquakes, and Tectonic Models to Identify Seismic Quiescence Zones

Vs30 Spatial Variations: Investigating Vs30 Variability in Seismically Quiescent Areas to Assess the Probability of Future Earthquakes

Practical Applications in Seismic Hazard Assessment: Using Vs30 Data to Predict Seismically Prone and Low-Risk Areas

Enhancing Seismic Models: Integrating Vs30 Data to Improve the Accuracy of Seismic Hazard Predictions

Crisis Management and Structural Resilience: Utilizing Vs30 Maps to Design Earthquake-Resistant Structures. Integrating the Vs30 spatial distribution map with seismic hazard assessments in Alborz and Tehran can help identify seismic gaps and predict earthquake-prone areas. The use of GIS, statistical analyses, and tectonic models enhances the accuracy of seismic hazard assessments and supports improved crisis management (Zare and purmohammad, 2023). As shown in (Fig. 1), the distribution of seismic events from 1957 to 2023 is based on shear wave velocity data.

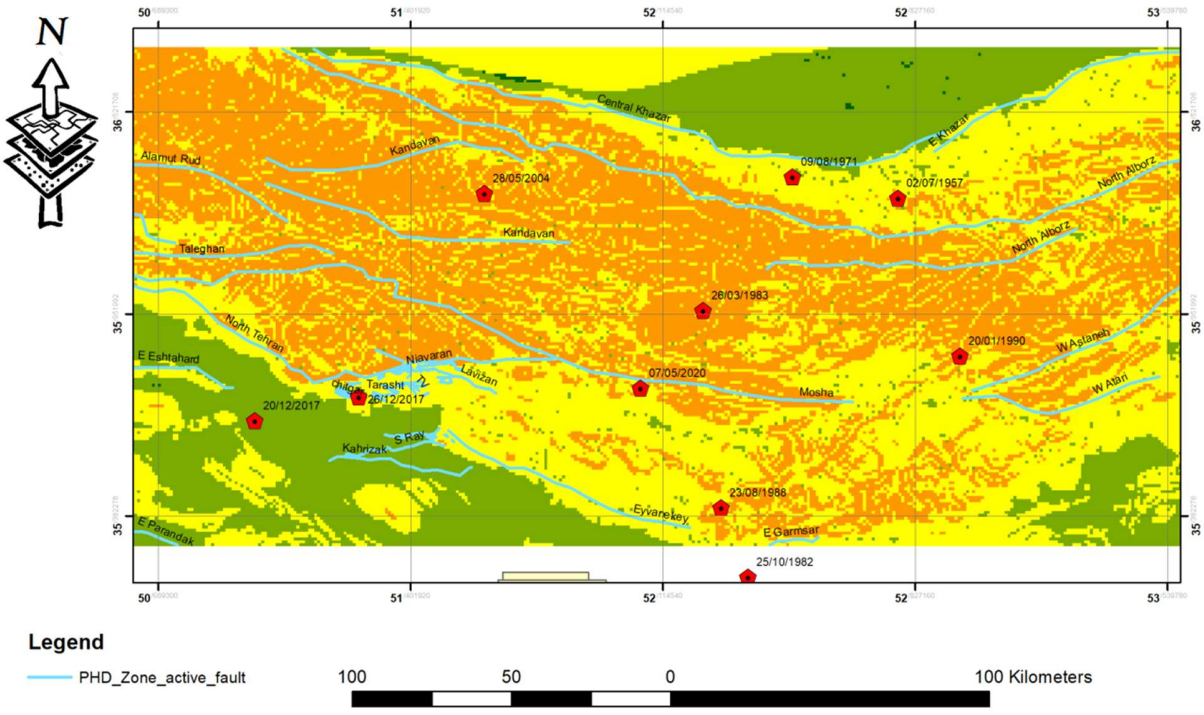

Figure 1. Location map of seismic events from 1957 to 2023 in the study area according to shear wave velocity data

Anbazhagan applied the HVSR method using a comparative analysis with various methods such as: time period method, shear wave velocity changes up to a depth of 30 m, spectral ratio, spectral curve fitting, and strong ground motion PGA, which gave a good result of combining and comparing multiple methods for site classification (Anbazhagan et al., 2019). Classified the site effect based on the PGA obtained from seismic events in Iran and Taiwan (Zare et al., 1999, Lee et al., 2001). With the progress of science and technology, some new approaches have emerged in recent years; in particular, the combination of multiple methods has been well applied (Xu and Wang, 2021). One of the surface wave analysis methods is the analysis and classification of the seismic site effect SSC, based on the shear wave velocity for 30 m above the soil or VS30, which is used for spatial classification (IsmetKanl et al., 2006). Using the SSC seismic site effect classification, the engineering properties of the soil can be presented using VS30 values in the study area and the NEHRP-1997 standard can be used, which introduces the average soil properties and shear strength based on the type of sediment. The NEHRP-1997 standard includes seismic bedrock with values greater than 1500 to 3000 m/s as a seismic indicator, while values of 400 to 700 m/s are considered engineering and hydrological bedrock (MunaffNaji et al., 2020). Presented in the table 1.

Table 1. SSC Site Effect Classification based on NEHRP-1997 classification (MunaffNaji et al., 2020) and (Aung, 2015)

N30	VS30 (m/s)	General Description	Ground Type Classification
-	> 1500	Hard Rock	A
-	760–1500	Rock	B
> 50	360–760	Very Dense Soil and Soft Rock	C
15–50	180–360	Stiff Soil	D
< 15	< 180	Soft Soil	E

The SSC site effect is the surface damage of the earthquake event within the PGA ground motion range, and the difference in site conditions will directly lead to different degrees of damage due to the earthquake. Therefore, researchers focus on the site effect under the influence of PGA ground motion and its strong vibrations (Xu and Wang, 2021). According to the table proposed by the US Geological Survey (PGV correlation with instrument intensity), which is used to create Shake Maps worldwide, the correlation between PGA ground motion data and PGV ground velocity isozone with the earthquake intensity scale (Mercalli) and consequently the modified Mercalliisozone MMI can be established as follows (Özener et al., 2018). Presented in the table 2.

Table 2. Correlation of PGV with Instrumental intensity (Özener et al., 2018)

PGV (cm/s)	Instrumental Intensity (MMI)	Recorded vibration (Shake)	Possibledamage
< 0.1	I	Not felt	None
0.1–1.1	II–III	Weak shaking	None
1.1–3.4	IV	Light shaking	None
3.4–8.1	V	Moderate shaking	Very light
8.1–16	VI	Strong shaking	Light
16–31	VII	Very strong shaking	Moderate
31–60	VIII	Severe shaking	Moderate to heavy
60–116	IX	Violent shaking	Heavy
> 116	X–XII	Extreme shaking	Very heavy

The maximum probable earthquake is defined as the largest earthquake that can occur in a study area due to fault movement. By calculating this magnitude and considering the distance between the construction site and the existing active fault (seismic source), the maximum horizontal acceleration generated by fault movement at the construction site can be predicted. Specifically, an earthquake with a return period of 475 years is used as a reference event, representing the maximum magnitude that a seismic source is capable of producing. This risk level, corresponding to a 475-year return period, is adopted as the design earthquake in the 2800 standard. By estimating the maximum seismic potential of the fault and the distance between the construction site and the active fault in the region, the maximum horizontal ground acceleration transmitted from fault movement to the site can be predicted. Additionally, the length of the fault rupture in future earthquakes can be estimated. The relationship between the surface rupture length of a fault and the earthquake magnitude is based on the fact that an earthquake involves longitudinal movement along a portion of the fault length. It is also commonly accepted that the rupture length (L) corresponds to a percentage of the total length of the active fault. Consequently, various researchers have developed models considering different regions, fault focal mechanisms, minimum probable magnitudes, and other factors (Zare and purmohammad, 2023).

2.1. Geographical Location of the Study Area

the Tehran and southern Central Alborzregion, covers a rectangulararea with the following coordinate:Latitude ranging from 35.3° to 36.7°degrees and Longituderanging from 50.6° to 53.6°.As shown in (Fig. 2), the stratigraphy of Tehran reveals the geological layers of the study area.

2.2. Tectonics of the study area

The continental crust of Iran underwent secondary folding and fracturing during the Hejaz or Pan-African tectonic phase (600 to 1000 million years ago), which also affected Saudi Arabia. Subsequently, the continental crust experienced deep folding and fracturing, resulting in raised and sunken sections (Agha Nabati, 2004). (Berberian and Yeats, 2001) suggests that the Tehran area, located in the southern foothills of the central Alborz Mountains, represents the northernmost depression of central Iran. The Alborz Mountains north of Tehran consist of east-west folds and thrusts that are superimposed and pushed outward (north and south) from the center of the Alborz range. The intensity of deformation reaches its maximum along the northern Caspian fault (Berberian, 1976b) and southern North Tehran fault (TChalenko, 1974) boundaries, with the Alborz highlands thrust onto the Caspian coastal plain to the north and the Tehran plain to the south, respectively. According to (TChalenko, 1974), Alborz seismicity is characterized by short-term periods of activity, where earthquake occurrences in one area coincide with quiescence in another. The duration of concentrated activity varies from approximately 4 years in the northwestern part to 12 years in the northeastern part. (Berberian et al., 1974), report that faults on the southern slopes of the Alborz act as southward thrusts, while those on the northern slopes act as northward thrusts. The fault zone between northern Iran and Eurasia on the northern slope of the Alborz is overlain by the Shemshak Formation, which exceeds one kilometer in thickness (Berberian and ambraseys, 1976a). According to the Iranian tectonic seismic map, most earthquakes in the Alborz region are shallow, although some are of intermediate depth. During the 20th century, the eastern part of the Alborz has been more seismically active than the western part.

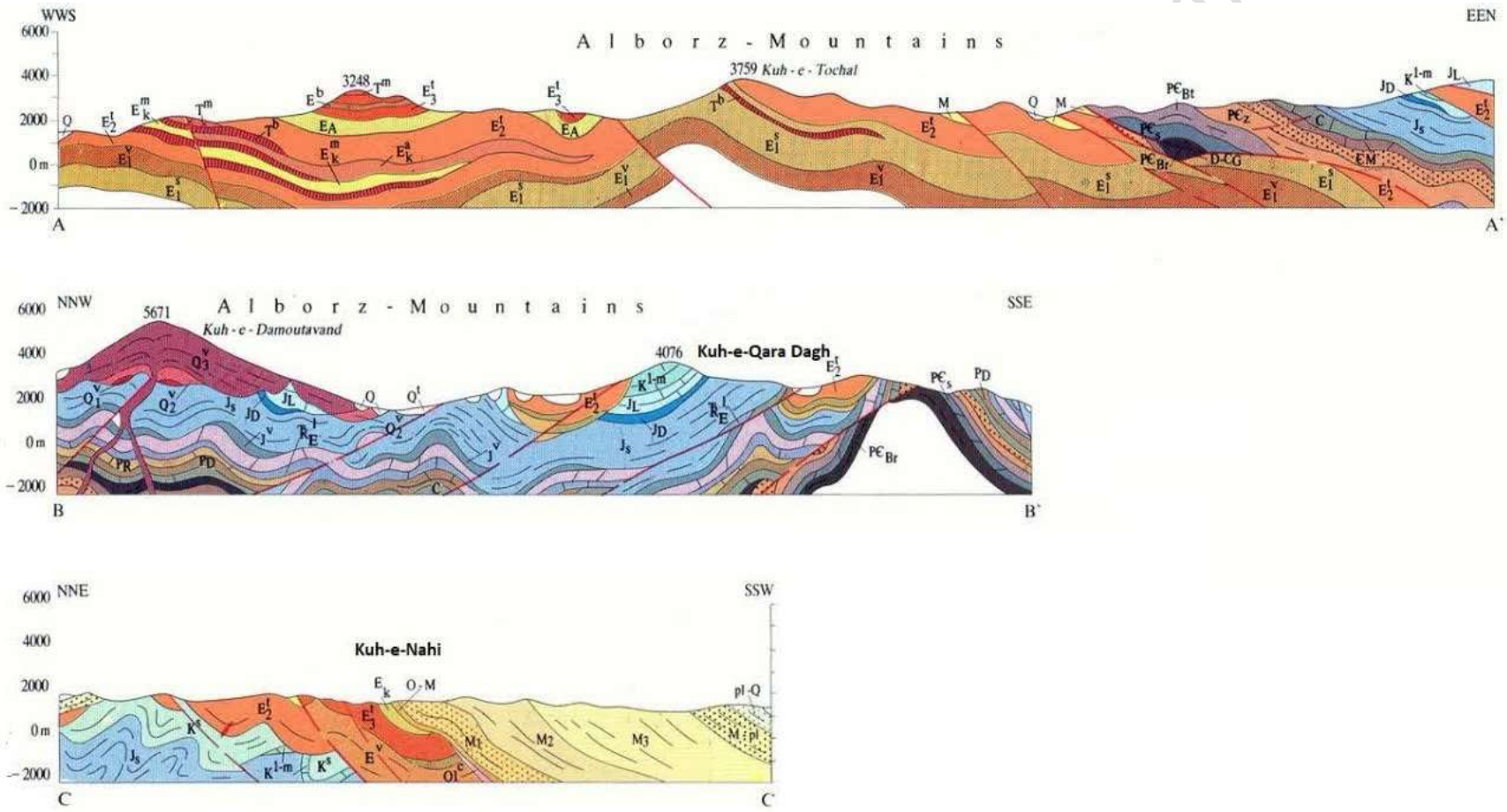

Figure 2. Tehran Stratigraphy

2.3. Faults, Study Area

TChalenko et al. (1974), Barbarian (1976-1981), and Ghorashi and Arzhang (1979), by studying the Quaternary faults of Tehran, have classified them as seismic and hazardous due to their young age and significant length in the Tehran area. They are divided into three groups, Presented in the table 3:

- Minor Faults - shorter than 2 kilometers: These faults are not seismic, but they can slip and displace due to the release of elastic energy along neighboring faults.
- Medium Faults - with lengths between 2 to 10 kilometers: These faults are sources of small tremors but are not seismic; however, due to the occurrence of large earthquakes nearby, they may slip and displace.
- Main Seismic Faults - longer than 10 kilometers: Young faults that cut through the alluvial deposits of Tehran's A, B, and C type sediments. The young age and great length of these faults make them seismic and hazardous within the Tehran area. The movement of these faults will cause high-magnitude earthquakes, which are introduced in the table

Table 3. Main Seismic Faults longer than 10 kilometers in the Tehran area(Berberian and yeats,1999)

Name	Type	Strike	Dip	Length (km)	Location
Mosha	Thrust - Active	East-Southeast to West-Northwest	North (35°–75°)	400	From southwest of Shahrud to Taleghan
North Tehran	Thrust - Active	East-West to East-Northeast	North (30°–80°)	75	From Lashkarak Valley (northeast Tehran) to Kazemabad (north of Tehran-Karaj Highway) and Karaj
Niyavaran	Thrust	East-Northeast to West-Southwest	North (15°–60°)	18	From Muradabad (west) to Bagh-e Bahai (east)
Talu Lower	Thrust	Northwest-Southeast	Southwest (35°)	13	From Talu Lower Village to the northern edge of Tehran-Abali Road
Mahmoudieh	Thrust	East-West	South	11	From Mahmoudieh (northeast of Vanak) to Chamran Highway (intersection with Valiasr Street)
Shian&Kosar	Thrust	East-West	South & Southwest	Shian: 3, Kosar: 13	North of Tehran Pars and Shian (Kosar Fault likely extends westward to Shian Fault)
North Ray	Thrust	North & Northwest of Ray City	Northward Thrust	16.5	Forms a weathered wall near Azimabad, north and northwest of Ray
South Ray	Thrust	---	Northward Thrust	18.5	Weathered walls south of the ancient hill (TappehGhar) in Qaleh No Village

Name	Type	Strike	Dip	Length (km)	Location
Kahrizak	Thrust - Active	East-West	Strike-slip with thrust component	40	From Sultanabad Village (west) to Kahrizak and Zalemabad Village (east)
Garmsar	Thrust - Active	East-West	North	70	From north of Garmsar to Pishva Fault in southeast Varamin
Pishva	Thrust	North 130° East	Northeast	34	Southeast of Varamin, at the mountain-plain boundary
Parchin	Thrust	Northwest-Southeast	North	---	South of Parchin, at the boundary between HezarDarreh Formation and the plain
Taleghan	Thrust	East-West	South	60	
Ivanaki	Thrust	Northwest-Southeast	North	75–80	Extends northwest-southeast, overlapping with Parchin Fault
Kandovan	Thrust	East-West to West-Northwest	---	75	
Eshtehard	Thrust	East-West	North	61	
Robat Karim	---	East-West	Limited seismicity data	90	Located in southern Tehran Province

2.4. Earthquakes in the Study Area

The study area has experienced both historical and instrumental earthquakes. Historical earthquakes are those that occurred before 1900, as documented by (Ambraseys and Berberian, 1976) and (Berberian and yeats, 1999).these have been provided for the study area (Seismic Map of Iran, Geophysics Institute). Presented in the table 4 to 6.

Table 4. Instrumental Earthquakes, Earthquake Catalog from the Tehran University Geophysics Institute IRSC (31/12/2022)

Time Period	M < 3.9	M 4–4.9	M 5–5.9	M 6–6.9	M ≥ 7
01/01/2006–31/12/2011	406	9	-	-	-
01/01/2012–31/12/2022	734	31	3	-	-

Table 5. Instrumental Earthquakes, Earthquake Catalog from the United States Geological Survey USGS (31/12/2022)

Time Period	M < 3.9	M 4–4.9	M 5–5.9	M 6–6.9	M ≥ 7
02/07/1957–31/12/2022	77	91	22	3	-

Table 6. Instrumental Earthquakes, Earthquake Catalog from the IIEES Seismology Research Center (12/31/2022):

Time Period	M < 3.9	M 4–4.9	M 5–5.9	M 6–6.9	M ≥ 7
01/01/1930–31/12/1959	-	22	15	1	1
01/01/1960–31/12/1979	-	19	1	-	-
01/01/1980–31/12/1999	8	24	6	1	-
01/01/2000–31/12/2022	1108	58	3	1	-

2.5. Seismic hazard estimation in the study area

Calculation of Empirical Relationships between Mb, MN, and Ms: In the Gutenberg-Richter relation, earthquake occurrence is described by the relationship between log (N) and magnitude (M). For events with M ≥ 4 on the Richter scale, the empirical relationship for the studied region was derived from each catalog using these relations. Since different catalogs report magnitudes using different units, the magnitudes were standardized to a common unit to determine the return period of events consistently. The magnitude unit used in this study is Ms, which serves as the basis for the return period evaluation methods. Presented in the table 7 and table 8.

Table 7. Relationship between different magnitudes for standardization with magnitude Ms Based on the above table and plotting the trend of seismic event occurrences based on magnitude Ms, the following relationships were obtained

Relationship	Condition	Formula
1	$Mb \leq 5$	$Ms = 1.14\ Mb - 1.136$
	$5 < Mb < 7$	$Ms = 0.334\ Mb^2 - 1.93\ Mb + 5.831$
2	$ML \leq 5$	$Ms = 0.671\ ML + 0.879$
	$5 \leq ML < 7$	$Ms = 0.272\ ML^2 - 1.641\ ML + 5.711$
3	$1 \leq ML \leq 6.2$	$MN = ML$

Based on these relationships, the frequency-magnitude distribution for Ms ≥ 4 in the study area was derived for each catalog:

Table 8. Relationship between frequency and magnitude Ms, and the number of seismic events in the study area for the catalogs

Catalog	Magnitude	Frequency-Magnitude Relationship
IIEES	Ms ≥ 4	Log(N) = 3.99788 + 0.00085(M)
IRSC	Ms ≥ 4	Log(N) = 3.74696 - 0.00022(M)
USGS	Ms ≥ 4	Log(N) = 4.06238 - 0.0052(M)

2.6. Gutenberg-Richter Relationship

This method, proposed by Gutenberg-Richter in 1956, shows a linear relationship between the cumulative frequency of earthquakes Nc and the magnitude M. By using this simple relationship, it is also possible to obtain the relationship between seismicity and its related coefficients (coefficients a and b) by performing a suitable classification for the magnitude of earthquakes.

$$\text{Log}\,(Nc)=a-bM \quad \text{(Eq1)}$$

In this context, Nc represents the cumulativefrequency of earthquakes[1] occurring during the study period for an earthquake of a specific magnitude, a is the seismicity parameter of the region, which depends on the number of earthquakes occurring in the region, b is the seismicity parameter of the region, which depends on the tectonic status of the region. The higher the value of a, the greater the number of events in the region in the desired time interval. The value of b is inversely related to the amount of accumulated stress in the region, and its low value indicates a high ratio of large to small events in the region, the value of b is usually between 0.5 and 1 (GhodratiAmiri, 2007). According to the limitation of the Gutenberg-Richter relation, the results are acceptable for the time interval when the seismic data are homogeneous and continuous (systemic seismic events) and their Msmagnitude range is between 3.4 and 5.1 (for irsc, a magnitude in the range of 3.6 to 4.5). Based on the plot of Log(Nc) values and Ms values like that and according to equation Eq1, we draw the graph for each of the catalogs and introduce the best linear relationship fitted to it as the Gutenberg-Richter relationship of the range.

To calculate the Gutenberg-Richter relationship with a focus on magnitude completeness (Mc), ensure that earthquake catalog is statistically reliable above a certain magnitude threshold. In Accordance with Gutenberg-Richter Law, This assumes an exponential distribution of magnitudes above the completeness threshold (Mc), (Taroni, 2023).

Estimating Magnitude of Completeness (Mc): A recent and robust method is based on random variable transformation, which improves upon traditional exponentiality tests. Here's the procedure: 1. Select a threshold magnitude M 2. Subtract M from each magnitude in the catalog:

[1]Cumulative frequency of earthquakes: First, seismic events are categorized based on magnitude, from the smallest to the largest. Then, for each interval, the number of events is summed with the number of events in the previous interval, and this cumulative total is considered as Nc for that interval. This process is repeated until reaching the first row, which corresponds to the smallest magnitude interval.

$X_i = M_i - M$ 3. Transform pairs of magnitudes using: $Zi = X_i / (X_i + X_{i+1})$, This yields values that should follow a uniform distribution if the original magnitudes are exponentially distributed. 4. Apply the Kolmogorov–Smirnov test to check for uniformity. 5. If the test passes (e.g., p-value ≥ 0.1), then M is considered the magnitude of completeness. Otherwise, increase M and repeat. This method is particularly useful when catalogs contain events with different b-values, which can distort traditional exponentiality tests (Taroni , 2023). Presented in the table 9.

Table 9. Gutenberg-Richter relationship (with spatial and temporal correction of the parameter a).

Catalog	Time Period	a	b	Equation	Eq. No.
IIEES	1930–2019 (89 years)	0.839	-0.504	Log(Nc) = 0.839 – 0.504 Ms (Eq2)	(Eq2)
IRSC	2006–2020 (15 years)	5.335	-1.675	Log(Nc) = 5.335 – 1.675 Ms (Eq3)	(Eq3)
USGS	1957–2019 (62 years)	2.202	-0.928	Log(Nc) = 2.202 – 0.928 Ms (Eq4)	(Eq4)

2.7. Poisson Model for the Study Area

Among several distribution characteristics, temporal distribution characteristics of earthquakes provide the most crucial information on the temporal patterns of past seismicity. Identification of such patterns is required for seismic hazard, forecast studies and also simulation of future seismicity. The confusion of how to model the past temporal patterns does limit further development:. Though the Poisson model is routinely used in hazard modeling (Karaca, 2024).Based on the final relationships obtained from the modified spatial and temporal Gutenberg-Richter model, the probability of an earthquake with a magnitude of Ms occurring in t years can be obtained using the Poisson model. In the Gutenberg-Richter model, the effective factor of the structure's life (time) is not involved, but in the Poisson model, this factor plays a fundamental role.

$$Pt=1-\exp(-Tt) \text{(Eq5)}$$

$$t = 5,10,15,20,25,50,100,150,200,250,500,1500,2000 \text{ (year)}$$

Using the above relationship, we determine the probability of an earthquake with a magnitude of Ms occurring in the study area over a period of 5 to 2000 years. Presented in the table 10.

Table 10. Probability of earthquake occurrence with magnitude Ms in the time period of 5 to 2000 years.

Eq. No.	Catalog	Time Period (Years)	Probability (%)	Magnitude Range (Ms)
(Eq2),(Eq5)	IIEES	5	1–10	5–7
		10	1–19	5–7.5
		15	1–27	5–8
		20	1–34	5–8
		25	1–40	5–8
(Eq3),(Eq5)	IRSC	5	≤0.5	5–6
		10	≤1	5–6
		15	≤1.5	5–6
		20	≤1.8	5–6.5
		25	≤2.25	5–6.5
(Eq4),(Eq5)	USGS	5	≤1.8	5–7.5
		10	≤3.5	5–8
		15	≤5.3	5–8
		20	≤7	5–8
		25	≤8.7	5–8

In order to provide a step-by-step explanation of the methodology used and to establish a clear connection between the figures and the content of the text, a flowchart of the conceptual process is presented as follows.As shown in (Fig. 3), the conceptual framework of this study illustrates the key components of the research approach.

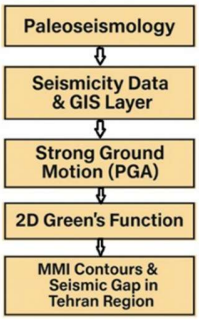

Figure 3. Conceptual Framework in this Article

3. Earthquake Hazard Assessment using Deterministic Method

3.1. Calculation of the earthquake return period

Evaluating the maximum ground motion acceleration risk for faults in the study area, based on deterministic earthquake risk estimation, requires estimating the maximum earthquake magnitude (Mmax) and determining the most appropriate relationship between ground motion and the estimated return period, slip rate, and activity of each fault segment. Since paleoseismological data

for the study area are unavailable, we rely on event statistics derived from the seismic catalog of the region. Subsequently, using the Gutenberg-Richter preliminary and empirical methods, we calculate the return period for the probability of an earthquake, as well as the Poisson model probability of an earthquake with a magnitude of Ms occurring within t years (90 years).

3.2. Estimation ofMaximum Earthquake or Mmax:

A study of seismicity in a region determines the priority of the next event in which part of the study area will cause a probable large earthquake, and by categorizing them; the priority of the absence of seismicity in the area can be determined. To determine the seismic hazard, the seismicity power of the fault in the area must be determined. The seismicity power of the fault is related to the ruptured length, the amount of fault displacement, and the maximum probable earthquake or maximum credible magnitude in an area. Given the faults in the region and the very long length of some of them, the probability of rupture of more than 50% for them in a future event can be probable. This value of 50% as the best fault rupture area is derived from the articles introduced in this study.The maximum probable magnitude Mmax, calculated by the magnitude-length relationship in the study area without regional segmentation, is presented in the table below. Presented in the (table 11.) For this purpose, a surface description is defined as the rupture surface, which is the amount of fault length that is active and has seismic potential (Zare et al., 2020).As shown in (Table 12.), key considerations for faults and seismic capacity are highlighted according to the IAEA guidelines.

Table 11. Maximum possible magnitude for major faults with lengths greater than 10 kilometers in the study area.

Fault	Length (km)	Mmax (Ambraseys& Melville 1982)	Mmax (Slemmons 1977)	Mmax (Norouzi&Mohajer-Ashjaei 1978)	Mmax (Zare 1995)
Ivanaki	80	6.9	6.9	7.0	6.7
Kahrizak	40	6.5	6.6	6.7	6.1
North Ray	16	5.9	6.2	6.3	5.3
South Ray	20	6.1	6.3	6.4	5.5
Pishva	34	6.4	6.5	6.6	6.0
Robat Karim	90	7.0	7.0	7.1	6.9
Mosha	400	7.9	7.7	7.7	8.2
North Tehran	75	6.9	6.9	7.0	6.7
Niavaran	18	6.0	6.2	6.4	5.4
Taleghan	60	6.7	6.8	6.9	6.5
Kandovan	75	6.9	6.9	7.0	6.7
Eshtehard	61	6.8	6.8	6.9	6.5
Qasr-e Firuzeh	26	6.2	6.4	6.5	5.7
SorkhHesar	30	6.3	6.5	6.6	5.9

Table 12. Key considerations for faults and seismic capacity according to the IAEA Guide; Fault Classes: This table includes the definitions of classes used in the compliation of Quaternary faults, liquefaction features, and deformation.

Class Category	Definition
Class A	Geologic evidence demonstrates the existence of a Quaternary fault of tectonic origin, whether the fault is exposed for mapping or inferred from liquefaction or other deformational features.
Class B	Geologic evidence demonstrates the existence of a fault or suggests Quaternary deformation, but either (1) the fault might not extend deeply enough to be a potential source of significant earthquakes, or (2) the Currently available geologic evidence is too strong to confidently assign the feature to Class C but not strong enough to assign it to Class A
Class C	Geologic evidence is insufficient to demonstrate (1) the existence of tectonic faults, or (2) Quaternary slip or deformation associated with the feature.
Class D	Geologic evidence demonstrates that the feature is not a tectonic fault or feature; this category includes features such as demonstrated joints or joint zones, landslides, erosional or fluvial scarps, or landforms resembling fault scarps, but of demonstrable non tectonic origin.

3.3. Determining the most appropriate ground motion magnitude relationship

Quantitative assessment of earthquake hazard requires estimating the amount of ground motion at a specified distance from the location of an earthquake of a given magnitude. This estimation is usually done using attenuation relationships or attenuation relationships in which ground motion is a function of the magnitude of the earthquake and the distance from the site to the Seismic sources. Attenuation relationships express the decrease in the amplitude of ground motion with increasing distance from the Seismic sources(Zare et al., 2020).Therefore, the farther we are from the epicenter of the earthquake, the less intense the ground motion is felt. The extent of this reduction depends on factors such as geological conditions, the type of movement on the fault surface, etc. Some relationships obtained based on strong ground motion data: Douglas (2003) considers ground motion parameters to follow a logarithmic normal distribution and expresses it as a function of magnitude and distance from the seismic Seismic sources, which is calculated by the following relationship (Zaferani and Noorzad, 2013; Douglas, 2003):

$$\text{Log}(Y) = \text{Log}\,[b1F1(M) + F2(R) + F3(M,R) + F4(pi) \ldots. + e] \qquad \text{(Eq6)}$$

Where Y is the strong ground motion parameter, F1(M) is a function of magnitude, F2(R) is a function of distance R, F3(M,R) is a combined function of magnitude and distance, and F4(Pi) is a function of the effect of other earthquake parameters including the wave path, the effect of the site and structure, and e is a random error variable. in an article titled: “Simulation of strong ground motion and presentation of mitigation relations for the Bushehr nuclear power plant site based on the finite fault stochastic method,” introduced the changes in PGA with respect to the earthquake

moment magnitude Mw and the Joiner-Bohr distance Rjb as follows (Hassankhani and Aram, 2017).

$$\text{Log (PGA)} = 1.437 + 0.7357M_w - 0.06147(M_w^2) + (-2.565 + 0.207M_w)\,\text{Log}_{10}\left((R_{jb}^2 + 6.65)^{0.5}\right) \quad \text{(Eq7)}$$

In seismic anechoic, the concept of Bohr distance is not used directly, but some studies have investigated the relationship of the physical principles associated with the Bohr model to the propagation of seismic waves. Seismic anechoic refers to areas where no significant seismic activity has been recorded or where large earthquakes have not occurred for long periods of time (Bommer and Akkar, 2012). Bohr Distance Relationship with Seismic Absence:

Modeling the Behavior of Tectonic Stresses: In some studies, quantum mechanical principles such as the Bohr radius are used to investigate the accumulation and release of tectonic stresses in seismically inactive areas. Analysis of the Earth's crustal structure: The concept of Bohr distance can be used to investigate the microscopic structure of geological materials and their effect on the propagation of seismic waves in less active areas. Relationship with wave theories: In some seismic models, physical principles similar to the Bohr model are used to analyze the propagation of P and S waves in the Earth's layers. Possible applications in seismicity assessment (Gupta, 2013):

Analysis of material behavior under high pressure conditions: Studying the atomic structure of materials in the Earth's crust to assess their effect on the propagation of seismic waves in seismically inactive areas Modeling of seismic wave propagation: Using physical principles similar to the Bohr model to analyze wave behavior in complex geological environments Connection with theories of tectonic rupture: Studying the effect of microscopic structures on fault rupture and earthquake occurrence in seismically inactive areas. Thus, although the Bohr distance is not directly used in seismicity, the physical principles associated with it can be used in modeling the behavior of tectonic stresses, analyzing the structure of the Earth's crust, and studying the behavior of geological materials. Various definitions have been proposed to express the distance of the construction site from the fault. These distances include the distance to the image of the fault plane Rjb, the closest distance to the rupture plane Rrup, the distance to the earthquake focus

Rhypo, and the distance to the seismic part of the fault Rseis. Based on this, the Joyner-Bohr-Fomal attenuation relationship has been introduced (Zare, 2017).

$$\text{Log PGA} = -0.038 + 0.216(M_{mid} - 6) - 0.777\text{Log}((R_{jb}^2+30.03)^{0.5}) \quad \text{(Eq8)}$$

Joyner-Boore Formalism is one of the important methods in seismology used for modeling ground motion and seismic hazard assessment. This method is developed based on accelerography data and analysis of fault distance to the earthquake location and is also used in studies related to seismic absence. The relationship of Joyner-Boore Formalism with seismicity assessment (Vats and Basu, 2023).

Ground motion modeling: This method uses seismic data to predict horizontal ground acceleration in different regions, Fault distance analysis to the earthquake recording site: The Rjb distance used in this model represents the shortest distance between the earthquake recording site and the fault surface and can play a role in seismicity assessment.

Investigation of seismicity-free areas: In areas where large earthquakes have not occurred for a long time, using the Joyner-Boore model can help identify areas with accumulated tectonic stresses.

Applications of Joyner-Boore Formalism in seismicity assessment (Vats and Basu, 2023): Seismic hazard analysis in less active areas: Using this model to investigate seismicity-free areas and the probability of future earthquakes.Modeling the seismic response of soil: Investigating the effect of geological characteristics on the propagation of seismic waves in areas with seismic absence.

Forecasting large earthquakes: Using seismic data and fault distance analysis to assess the probability of large earthquakes in the future. Therefore, the Joyner-Boore Formalism model is one of the important tools in seismic hazard analysis that can be used in assessing seismic absence and identifying earthquake-prone areas. This model helps to predict ground motion and assess seismic hazard by using seismic data and fault distance analysis. GhodratiAmiri introduced attenuation relationships for Iran using the model and different magnitude values in different seismic states of Zagros and Alborz-Central Iran, and introduced PGA-based attenuation relationships for magnitudes of 4.5 to 7.5 Richter in rock and soil beds at each horizontal and vertical distance (GhodratiAmiri et al., 2018).

Rock Bed (Alborz-Central Iran)

$$Ln\ (PGAH) = 4.15 + 0.623 * M_s - 0.960 * Ln(\ R) \qquad (Eq9)$$

$$Ln\ (PGAV) = 3.46 + 0.635 * M_s - 0.996 * Ln(\ R) \qquad (Eq10)$$

Soil (Alborz-Central Iran)

$$Ln\ (PGAH) = 3.65 + 0.678 * M_s - 0.950 * Ln(\ R) \qquad (Eq11)$$

$$Ln\ (PGAV) = 3.03 + 0.732 * M_s - 1.030 * Ln(\ R) \qquad (Eq12)$$

In the above relationship, Ms is the surface magnitude and R is the focal length (GhodratiAmiri et al., 2018).

The horizontal spectral acceleration reduction relationship of ground motion for northwest Iran was, for the first time, a suitable theoretical-experimental reduction relationship for the East Azerbaijan-northwest Iran region (Alpine Belt) as follows.

$$Log\ (PGA) = 2.62 + 0.35 * (M_w - 0.35) - 0.1 * (M_w - 0.35)^2 - (0.88 + 0.88*M_w) * Log(R) - 0.0078 * R \qquad (Eq13)$$

In the above equation, Mw or the magnitude of the torque and R Joyner-Bohr (the shortest distance to the surface image of the fault on the earth's surface in kilometers) are considered.

Article: Preparation of acceleration reduction relationship for the Iranian Plateau by updating the GhodratiAmiri reduction relationship, 2007, Acceleration reduction relationships for the seismic regions of Zagros and Alborz-Central Iran in rock and soil bed construction site conditions (GhodratiAmiri et al., 2018).

Rock Bed (Alborz-Central Iran)

$$Log\ (PGA) = 1.864 + 0.141*M_s - 0.614*Log® \qquad (Eq14)$$

Soil (Alborz-Central Iran)

$$Log\ (PGA) = 1.627 + 0.284*M_s - 0.930*Log® \qquad (Eq15)$$

In the above relations, the coefficients C1, C2, C3 related to the Alborz-Central Iran seismicity state for soil and rock beds are introduced in this study, PGA is the acceleration, Ms is the surface magnitude, and R is the focal distance (GhodatiAmiri et al., 2018).

Given that the Douglas relation has coefficients that are obtained from the regression of earthquake data and geotechnical samples, therefore, with the aim of standardizing the data, we use a more comprehensive relation of Donovan 1973, which was obtained based on the global average, in this study.

$$a = 1.1\ e^{0.5\ M(max)}\ (R+25)^{-1.32} \qquad \text{(Eq16)}$$

In the above equation, a is the maximum acceleration of gravity in g, which is calculated according to the Mmax of each fault, where R is the distance from the Seismic sourcesin km.

The interpretation and analysis of the seismic parameters table of Tehran and Alborz faults is presented in Table 13 as follows: This table contains seismic characteristics of various faults in Tehran and Alborz, which have been compiled from various studies. Key information in this table includes the fault length, magnitudes calculated by various studies, the maximum ground acceleration at the epicenter, and the seismic intensity at the epicenter (I_0) (GhodatiAmiri et al., 2018).

Analysis of the main parameters of the table: a) Fault length and its effect on earthquake magnitude, Longer faults (such as the 90 km Mosha fault and the 400 km North Tehran fault) are generally prone to larger earthquakes, because the fault length has a direct relationship with the amount of energy released during tectonic failure.Shorter faults, such as the North and South Rey faults, have lower magnitudes, but may cause destructive earthquakes in urban areas.b) Magnitude calculated by different studies, Different studies such as Ambrose (Norouzi and Mohajerashai, 1978) have provided different magnitude values for these faults, which indicate the uncertainty in seismic modeling. The Mosha Fault and the Talegan Fault have the highest magnitude values (7.9 and 6.7 and above), which indicate high seismic potential in the northeast Tehran region. c) Maximum ground acceleration at the epicenter, the ground acceleration value (cm/s^2) indicates the magnitude of seismic forces at the epicenter.

The Mosha Fault (815 cm/s²) and the North Tehran Fault (495 cm/s²) have the highest acceleration values, which indicate the strong seismic effect in the Tehran seismic region. d) Seismic intensity (I_0) at the epicenter, Seismic intensity values such as X (10), VIII+ (8.5) indicate the extent of destruction at the epicenter. The North Rey fault and the South Rey fault have high intensities, which indicate a potential risk of urban destruction in the southern and central regions of Tehran. Review of the largest historical earthquakes: Historical earthquakes associated with these faults have been in the range of 7.1 to 7.7 on the Richter scale. The largest earthquakes belong to the Kahrizak, North Rey, and Talegan faults, which can cause serious damage.

Seismic consequences and proposed measures: a) Seismic hazard analysis and strengthening measures, it is necessary to improve the design of urban structures in the area of high-risk faults such as North Rey and Mosha. Installation of early warning systems to reduce human losses in densely populated areas. Assessing critical infrastructure such as hospitals and power lines for resilience to large earthquakes.

b) Improving seismic data and more accurate modeling Combining GPS and InSAR data to examine more accurate fault slip rates., Using newer models such as PSHA (Probabilistic Seismic Hazard Analysis) to reduce uncertainty in the magnitude of future earthquakes. Therefore, this table provides an overview of the seismic hazard of Tehran and Alborz faults. Data analysis shows that the North Rey, Mosha, Kahrizak, and Talegan faults pose the greatest risk to Tehran. The use of early warning systems, urban resilience, and more accurate modeling can help reduce earthquake hazards in these areas (Ritz, et al., 2012).

Table 13. Determining the most appropriate strong ground motion equation for major faults with a length of more than 10 km in the study area

Fault	Length Fault	Ambrose and Melville 1982 (L = %50 LF)	Salmons 1977 (L = %50 LF)	Norouzi and Mohajeras hjai 1978	Zare 1995 or 1374 (L = %37 LF)	Maximum acceleration of gravity calculated at the	Largest historical event
Ivanki	80	6.9	6.9	7.0	6.7	495	7.6
Kahrizak	40	6.5	6.6	6.7	6.1	405	
North of Rey	16	5.9	6.2	6.3	5.3	300	7.7
South of Rey	20	6.1	6.3	6.4	5.5	315	7.2
Pishva	34	6.4	6.5	6.6	6.0	385	
Mosha	90	7.9	7.7	7.7	8.2	815	7.1
North of Tehran	400	6.9	6.9	7.0	6.7	495	7.1

Niavaran	75	6.0	6.2	6.4	5.4	315	
Talegan	18	6.7	6.8	6.9	6.5	448	7.7
Kandovan	60	6.9	6.9	7.0	6.7	495	
Ashthard	75	6.8	6.8	6.9	6.5	448	7.2
Qasrafirouzeh	61	6.2	6.4	6.5	5.7	340	
SorkhHesar	26	6.3	6.5	6.6	5.9	359	

Field evidence, seismicity, and geodetic data for defining the tectonic evolution of active faults in the western and central Alborz zones indicate that the structures of fault zones and their spatial distribution along the northern slope of the western and central Alborz zones are strongly influenced by the strain distribution process in the transpressional zone. Also, a study of the geometric-dynamical characteristics of the northern Alborz fault zone indicating the active parts in the fault zone has been introduced (Rashidi et al. 2023). The Alborz mountain range in northern Iran is part of the active and seismic Alpide belt, where assessing seismic hazards is crucial due to the region's history of large instrumental earthquakes and destructive seismic background. Moment rate estimation, which quantifies tectonic activity, offers a novel approach to understanding the energy potential of active tectonic regions. These faults have a seismic potential of Mw 6.5 and a gravity of ~0.5723. While previous studies have identified faults in northern Tehran as the greatest seismic risk, our findings suggest otherwise (Mohammadi Nia et al. 2023).

With the aim of providing a detailed discussion on how Probabilistic Seismic Hazard Analysis (PSHA) can complement the findings and this approach is included in the text as follows to be investigated in the context of Tehran and the central Alborz. As requested by the editor, it has led to improved hazard assessment in the study area.

Comparison of Probabilistic Seismic Hazard Analysis (PSHA) and Definitive Seismic Hazard Analysis (DSHA) in the Assessment of Seismic Absence in Tehran and Central Alborz:

Probabilistic Seismic Hazard Analysis (PSHA) and Definitive Seismic Hazard Analysis (DSHA) are the two main approaches in seismic hazard assessment. Both methods can help identify seismic absence in Tehran and Central Alborz, but they have important differences in the way data is processed and the risk assessment is performed.

The Role of PSHA in the Development of Seismic Absence Assessment: By considering seismic uncertainties, PSHA can help analyze seismic absence in Tehran and Central Alborz. This method includes: probabilistic modeling of earthquake occurrence based on historical data and seismicity

rates, analysis of the spatial distribution of tectonic stresses to identify areas with seismic absence, investigation of the impact of seismic absence on future seismic hazard using probabilistic models, and integration of seismic and geophysical data to increase the accuracy of seismic forecasts. Recent studies have shown that the use of PSHA based on physical models can increase the accuracy of seismic hazard assessment and better analyze the impact of seismic absence (Alikhanzadeh and Zafarani, 2023). Presented in the table 14.

3.4. Comparison of PSHA and DSHA in seismic absence assessment

Table 14. Comparison of PSHA and DSHA in Seismic Gap (Motaghed et al., 2023, Boostan and et al., 2015).

Feature	PSHA Probable	DSHA determination
Seismic hazard modeling	Based on the probability distribution of events	Based on a specific scenario
Considering uncertainties	Yes, including uncertainty in magnitude, location, and time of occurrence	No, only a specific scenario is considered.
Seismic analysis	Investigating the impact of seismic absence on future seismic hazard	Focus on major historical events
Application in Tehran and Alborz	Suitable for analyzing low-activity and seismically inactive areas	Suitable for investigating large earthquake scenarios
Accuracy in predicting seismic hazard	High due to taking into account uncertainties	Moderate due to limitations in the scenarios examined

PSHA can perform seismic absence analysis more accurately and identify areas with accumulated stresses due to the consideration of seismic uncertainties. In contrast, DSHA focuses more on historical large earthquakes and may not fully consider seismic absence.

Practical applications in Tehran and central Alborz: PSHA can help identify seismic absence areas and predict future seismic hazard. DSHA is suitable for investigating large earthquake scenarios and designing structural retrofitting. The combination of PSHA and DSHA can provide more comprehensive seismic hazard modeling.Therefore, PSHA, by considering seismic uncertainties, can perform seismic absence analysis more accurately and identify areas with accumulated stresses. In contrast, DSHA focuses more on historical large earthquakes and may not fully consider seismic absence. The combination of these two methods can provide more comprehensive seismic hazard modeling and help with crisis management and structural retrofitting (Motaghed et al., 2023; Boostan et al., 2015).

4. Determining potential earthquake Seismic sources in the study area

To investigate the seismicity of a region, it is essential to have an accurate understanding of the seismic characteristics of the region's tectonics and faults (both surface and subsurface) as earthquake seismic sources. These seismic sources can be classified as point, linear, area, or volume sources, depending on the level of knowledge and the ability to delineate them. The study area for this research encompasses the most significant part of Tehran Province. The data mining process was based on seismic events from 1957 to 2023 within the study area, focusing on events with a magnitude greater than 4 on the Richter scale, as detailed below Presented inthe table 15:
To better understand the events selected in this study, a map showing the locations of seismic events from 1957 to 2023 within the 2800 Plan area was used. As shown in (Fig. 4), seismic occurrences from 1957 to 2023 are mapped over the 2800 design area.

Table 15. Metadata of seismic events from 1957 to 2023 in the study area with a magnitude of more than 4

Center	MMI	UTC	Date	Depth	Mag	Long	Lat	HDF
Soleh Bon	VII	01:27:09	01/20/1990	24.5	6.0	52/954	35/832	1
damavand	V	04:07:19	03/26/1983	33.0	5.4	52/228	35/961	2
tehran	IV	21:24:32	12/26/2017	10.0	4.0	51/256	35/716	3
malard	V	19:57:38	12/20/2017	10.0	4.9	50/962	35/649	4
istgahrahahangarmsar	VI	05:30:47	08/23/1988	10.0	5.2	52/279	35/404	6
istgahrahahangarmsar	V	16:54:51	10/25/1982	33.0	5.4	52/355	35/208	7
damavand	V	20:18:22	05/07/2020	10.0	4.6	52/051	35/742	12
babol	VI	02:54:37	08/09/1971	20.0	5.6	52/481	36/337	17
babol	VII	00:42:26	07/02/1957	15.0	6.6	52/778	36/277	18
nowshahr	VII	12:38:44	05/28/2004	17.0	6.3	51/610	36/290	19

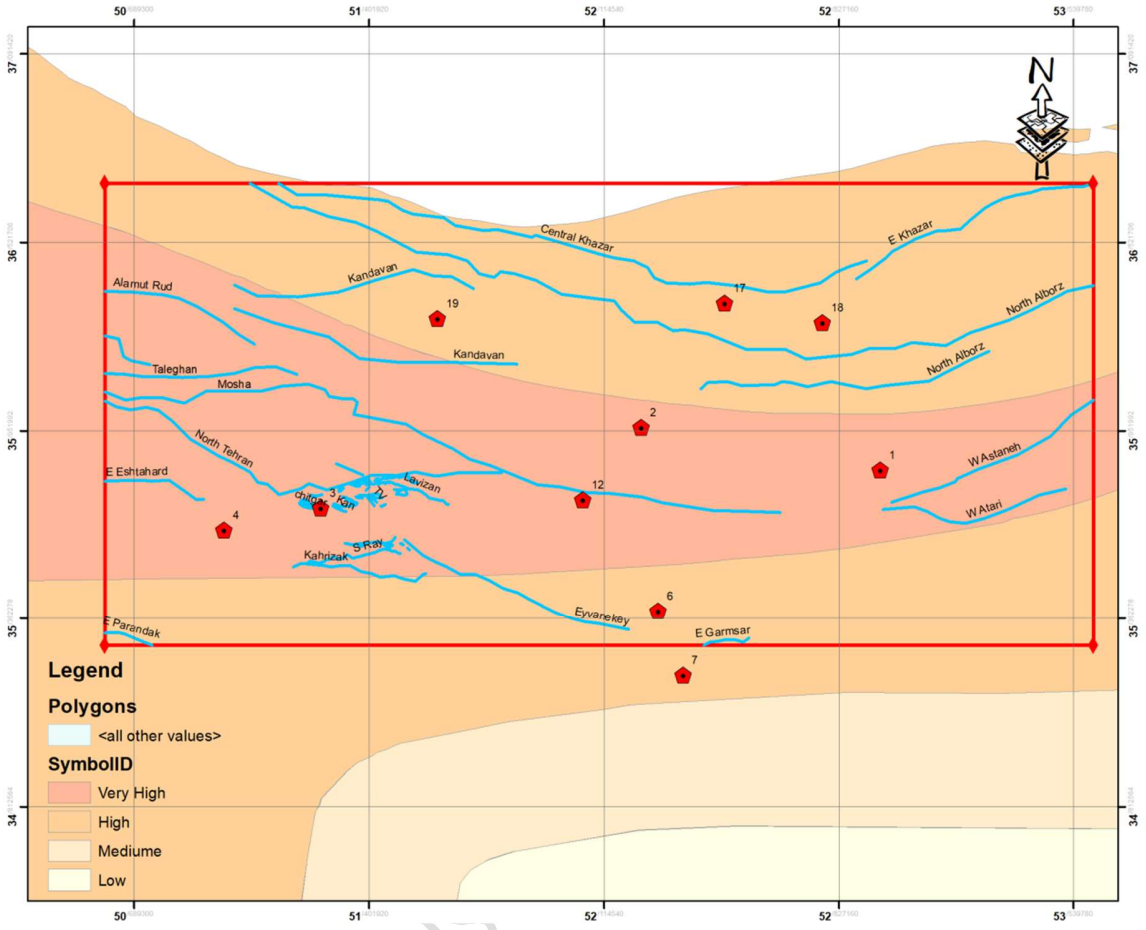

Figure 4. Location map of seismic events from 1957 to 2023 occurrences on the 2800 design area in the study area

Using the HDF metadata files generated by the USGS ShakeMap model, a two-dimensional raster layer was created to support seismic hazard analysis. This was accomplished by coding within a software environment to generate a point cloud, which was then used to construct a strong ground motion intensity matrix with spatial intervals of 50 x 50 meters. Subsequently, the descriptive information layer was saved as a TXT file and converted into conceptual layers representing the "MMI Seismic Intensity Zone, "PGA Strong Ground Motion Zone, and "PGV Ground Layer Velocity Zone. ArcGIS software and applied the kriging interpolation method. The key features of the resulting layers are as follows:

1) Determination of the isointensity zone based on the Modified Mercalli Intensity (MMI) scale and its correlation with faults in the study area to identify the rupture zone near the fault responsible

for the earthquake. 2) The study area within the identified zone is considered a potential site for future earthquake activity, which can be used to assess seismic quiescence and prioritize monitoring of upcoming events. 3) The calculated MMI values help identify the "causal fault" and elucidate the relationships between seismic events and their spatial distribution within the study area. 4) The study area was classified according to the presented zoning, with the northern part exhibiting very high relative risk and the southern part showing high relative risk. 5) These parameters are applied to the fault rupture zone and the distribution of strong ground motion at the surface, aiming to delineate the rupture zone and increase the probability of fault slip in the vicinity of the earthquake. This approach serves as a method for assessing seismicity and forecasting future events. Accordingly, the values assigned to these parameters can be used to identify areas prone to seismic activity.

As an example, Ozner, the rate of occurrence of earthquakes with a magnitude of 6 in the 250-year predictions. In this case, the maximum amount of strong ground motion that creates the greatest impact at the seismic site with an optimal distance of 15 km from the fault is equal to 0.168g, also the PGV parameter value for this example will be 10.5 cm/s and the PGD parameter value will have a displacement of 1.65 cm (Özener et al., 2018).

Quantification and validation of seismic absence beyond MMI and PGA data in the Alborz and Tehran regions:Seismic absence refers to areas where seismic activity is lower than expected. The assessment of these areas requires the use of multi-source methods that, in addition to Modified Mercalli Intensity (MMI) and Peak Ground Acceleration (PGA), also include geophysical data, tectonic stress modeling, and advanced seismic analysis (Tourani et al., 2024).

Data Processing Steps for Seismic Absence Quantification: Seismic and tectonic data collection involves reviewing historical earthquake catalogs to analyze areas with low seismic activity; using GPS and InSAR data to study changes in tectonic stresses; extracting b-values in different regions of Alborz and Tehran to identify seismic absences; and processing Vs30 data to investigate the effects of soil properties on seismic wave propagation.To investigate the active tectonics and the state of pre and post-seismic stress distribution of the source region, applied a combination of Coulomb stress change, b-value mapping, and Inferred Coulomb stress field reveals the E–W-striking (dextral) fault responsible for the first event and the NNE–SSW-striking (sinistral reverse) fault for the second event (Yazarloo et al., 2021).

Geophysical and numerical analyses: Use of Gumbel and Gutenberg-Richter models to analyze the distribution of seismic events, Investigation of mechanical properties of active and semi-active faults with tectonic models, Seismic fractal analysis to investigate temporal and spatial patterns of seismic absence

Criteria for defining seismicity:To determine seismicity, several complementary criteria need to be considered: Low b-value indicates areas where tectonic stresses have accumulated without seismic release, Areas with low seismicity rates compared to other active fault segments, Long distance from major historical earthquakes indicating long-term seismicity, Areas with stress changes without earthquake occurrence identified by GPS and InSAR data, Static instability of the Earth's crust estimated through tectonic stress analysis

Methods for validating and reproducible seismic absence

Comparison of Multiyear Data: Investigating seismic trends over the past 10 to 50 years to identify areas exhibiting seismic absence.Conducting correlation analyses between historical seismic data and changes in tectonic stresses. Multi-Source Seismic Hazard Modeling: Integrating peak ground acceleration (PGA), Modified Mercalli Intensity (MMI), b-value, GPS, and InSAR data to enhance the accuracy of seismic absence assessments. Employing multivariate probabilistic models to analyze the seismic behavior of low-activity regions. Geophysical Analysis and Crustal Resistance: Examining the effects of soil and rock properties on seismic wave propagation in areas characterized by seismic absence. Analyzing changes in the elastic properties of the crust and their relationship to seismic absence.

Applications of seismic vulnerability assessment in crisis management and urban planning:

Identifying areas prone to large earthquakes involves assessing seismic vulnerability and the accumulation of tectonic stresses. Optimizing urban design and structural retrofitting should be guided by the results of seismic vulnerability quantification. Additionally, predicting future seismic events requires the integration of multi-source data and probabilistic models. Therefore, quantifying and validating seismic vulnerability in the Alborz and Tehran regions necessitates multi-source data analysis, numerical modeling, and examination of tectonic stress variations. Employing methods beyond traditional measures such as MMI and PGA— including b-value analysis, GPS data interpretation, probabilistic modeling, and seismic fractal analysis—can

enhance the identification of vulnerable areas and improve seismic risk assessment (Bastami and Kowsari, 2014).

Uncertainties in data and methods—such as potential errors in seismic catalogs (IIEES, IRSC, USGS), interpolation techniques like kriging, and assumptions in reduction relations—are inherent in all seismological studies. In this work, these factors were not merely treated as assumptions but were applied according to the specific conditions of the problem, with careful consideration of their limitations. Indeed, our most significant achievement was compiling a collection of small cases that this topic could effectively address (Bastami and Kowsari, 2014).

Comparison of IIEES, IRSC and USGS seismic catalogs for Tehran and Alborz:

Analysis of different seismic catalogs can help identify discrepancies in data, catalog inconsistencies, and the influence of unmodeled parameters such as CMT (Centroid Moment Tensor) (Tourani et al., 2024).

Data availability discrepancies:

The Iranian International Institute of Earthquake Engineering and Seismology (IIEES) focuses on Iranian seismic data, particularly in active regions such as Alborz and Tehran. It includes smaller earthquakes that may not be recorded in international catalogs. The Iranian Seismological Center (IRSC) provides domestic seismic data, emphasizing local seismic networks. The USGS (United States Geological Survey) primarily focuses on larger earthquakes and global data. While it may not record some smaller earthquakes in Iran, it provides more accurate data for significant seismic events.

Catalog Inconsistencies: Differences in magnitude scales: The USGS typically uses Mw (Moment Magnitude), whereas the IRSC and IIEES may use ML (Local Magnitude) or Mb (Body-wave Magnitude). Differences in data processing methods: The USGS employs global models to analyze seismic data, while the IRSC and IIEES utilize regional models. Inconsistencies in event timing: Some earthquakes may be recorded in one catalog but not in another due to variations in the sensitivity of seismographic networks. The effect of un modeled parameters such as the Centroid Moment Tensor (CMT) is significant in analyzing the Iranian Seismological Center (IRSC) may not provide CMT data for smaller earthquakes, whereas the United States Geological Survey

(USGS) typically publishes this data for larger events. The absence of accurate tectonic stress modeling in some catalogs can result in discrepancies in seismic hazard assessments.

Therefore, the IIEES, IRSC, and USGS seismic catalogs each have their own strengths and weaknesses. IIEES and IRSC provide more accurate local data, but may record some larger earthquakes with less accuracy. USGS has global data and more advanced models, but may not record some smaller earthquakes in Iran (Tourani et al., 2024). Due to the large study area and to improve the quality of the output, (Fig. 3) Was presented as a summary map, including seismic faults and their spatial relationships in the study area. As shown in (Fig. 5) to (Fig. 7), the deterministic models illustrate the isoseismal zones (MMI) corresponding to earthquakes with magnitudes ranging from 4 to 6, including separate representations for magnitudes 4 to 4.9 (Fig. 5), 5 to 5.9 (Fig. 6), and 6.0 (Fig. 7).

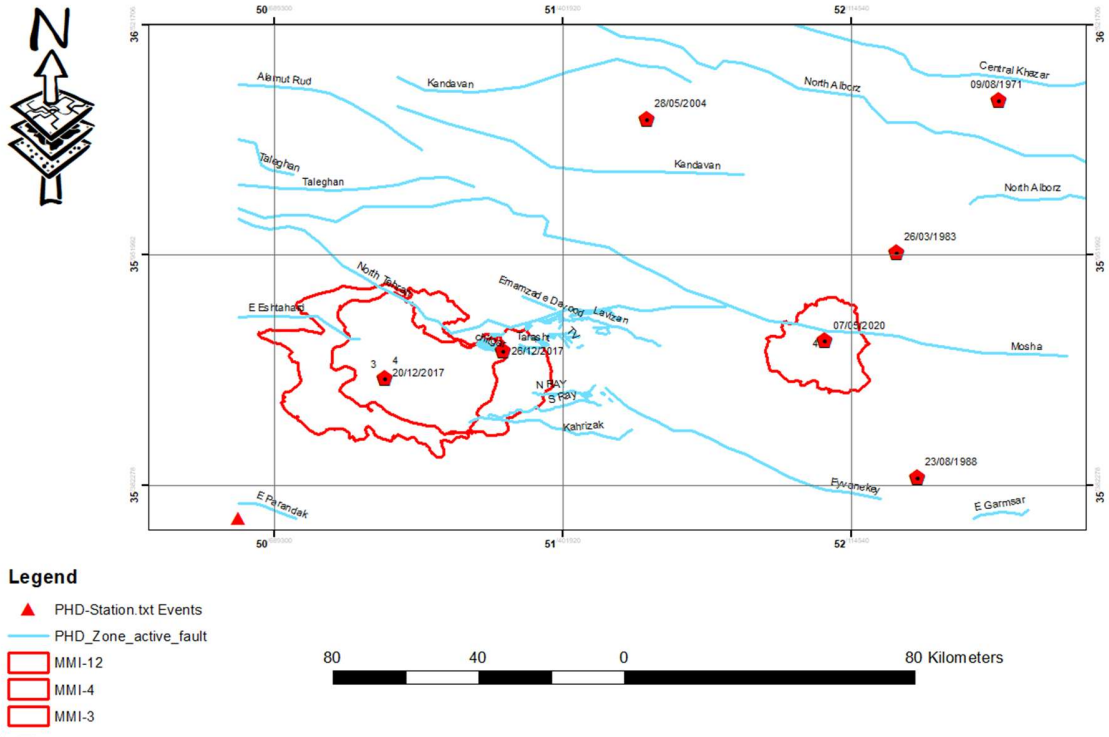

Figure 5. Deterministic model of the area source and the area of isointensity (MMI) of magnitude 4 to 4.9

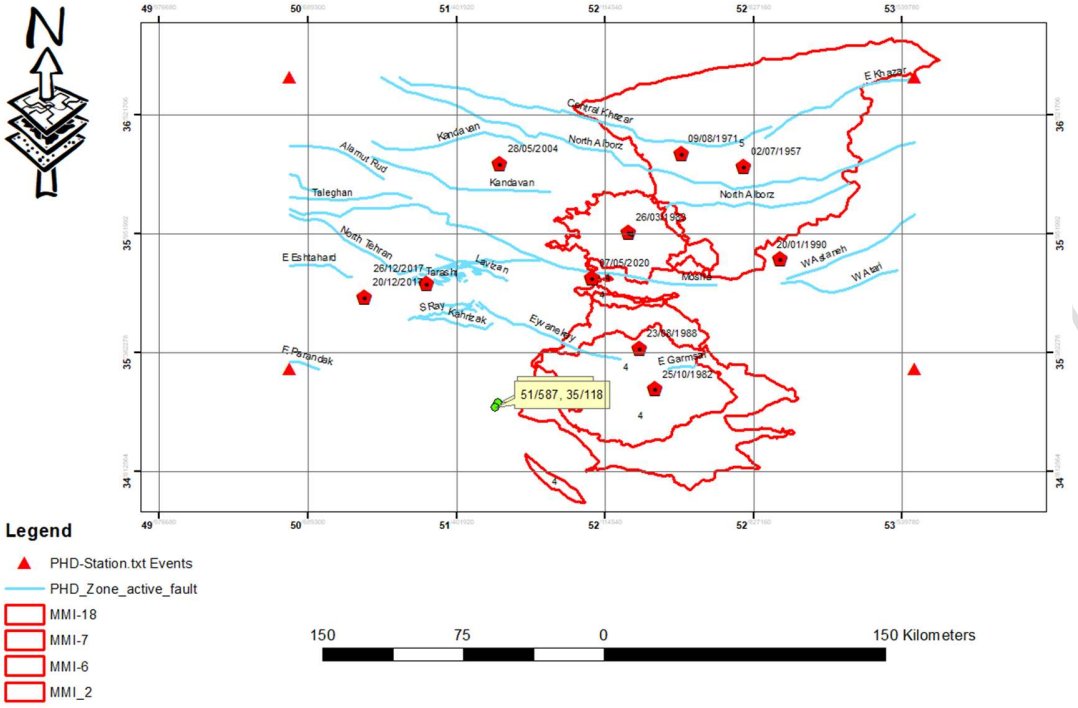

Figure 6. Deterministic model of the area source and the area of isointensity (MMI) of magnitude 5 to 5.9

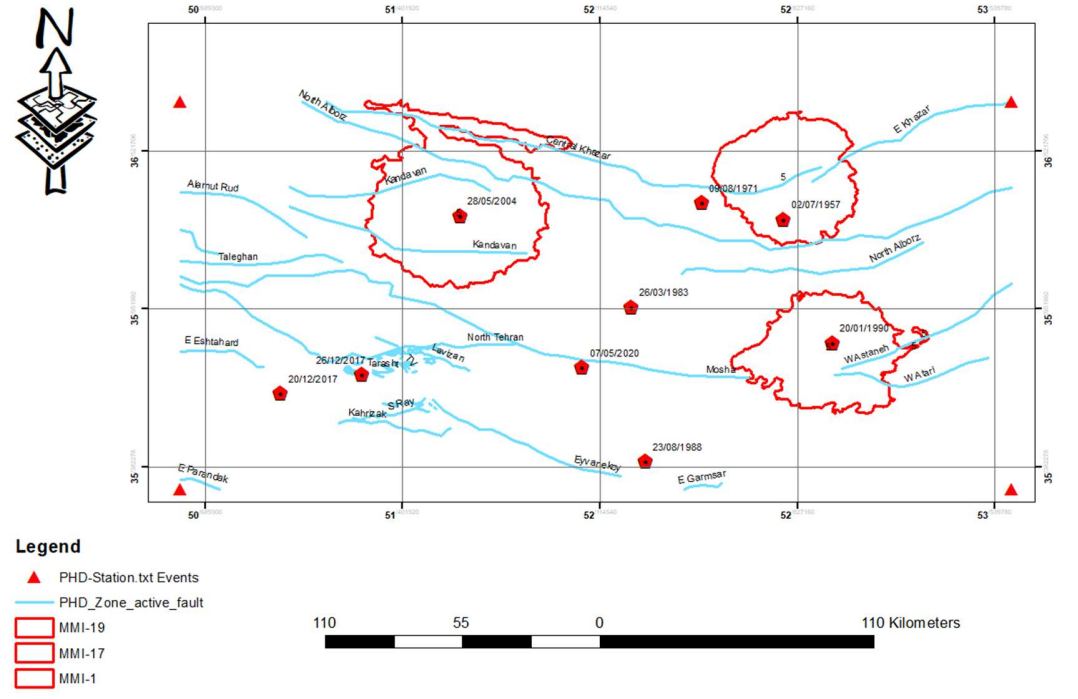

Figure 7. Deterministic model of the area source and the area of isointensity (MMI) of magnitude 6

5. Research Findings

Seismic Absence "A": To identify potential earthquake seismic sources in the study area.

After determining the MMI and isointensity zones for the Damavand earthquake on 26/03/1983, it appears that a 42 km-long segment in the eastern part of the Mosha fault was locked. According to the "Zare (1374) (L = 37% LF) relationship, can be assumed to have a maximum magnitude of MMax = 6.2 Richter. While part of this seismic absence occurred in the 17 km long segment of the Damavand - 07/05/2020 earthquake with a magnitude of 4.6 Richter (Fig. 9), there is still a segment of about 25 km long on the eastern part of the Mosha fault, which, according to the shown in (Fig. 8, 10, and 11, deterministic models present the isoseismal zones (MMI) for historical earthquakes in the region, including the 1983 Damavand earthquake with magnitude 4 (Fig. 8), the 2004 Nowshahr earthquake with magnitude 5 (Fig. 10), and the 1982 Garmsar earthquake with magnitude 4 (Fig. 11).

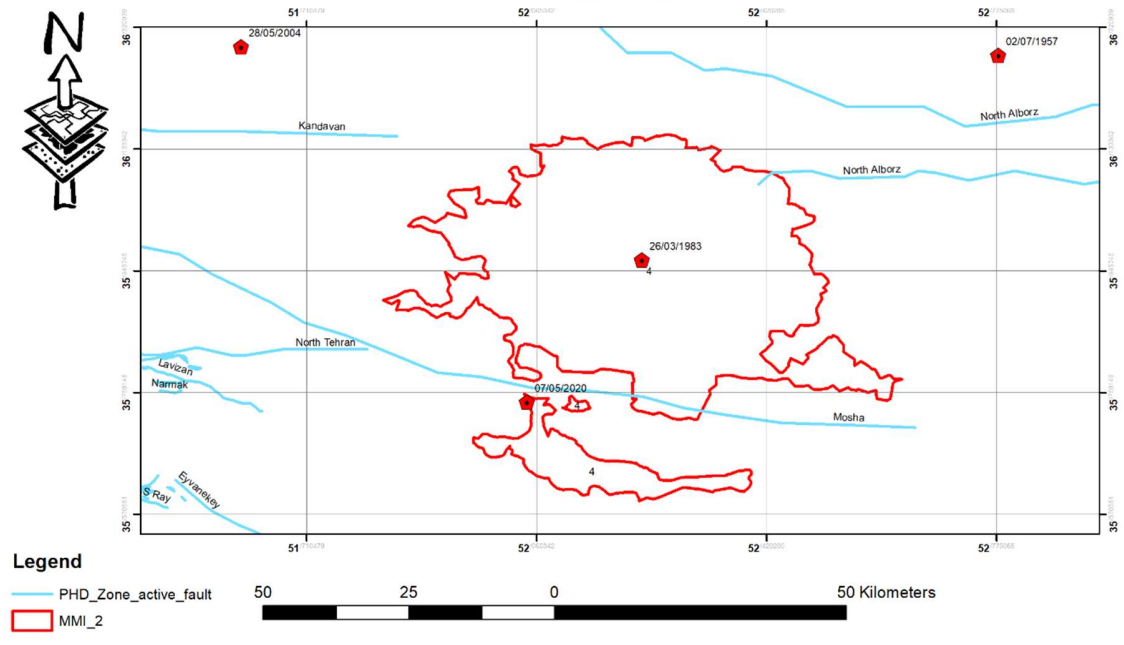

Figure 8. Definite model of zone Seismic sourcesand zone isointensity (MMI) of magnitude 4 for the Damavand earthquake - 03/26/1983

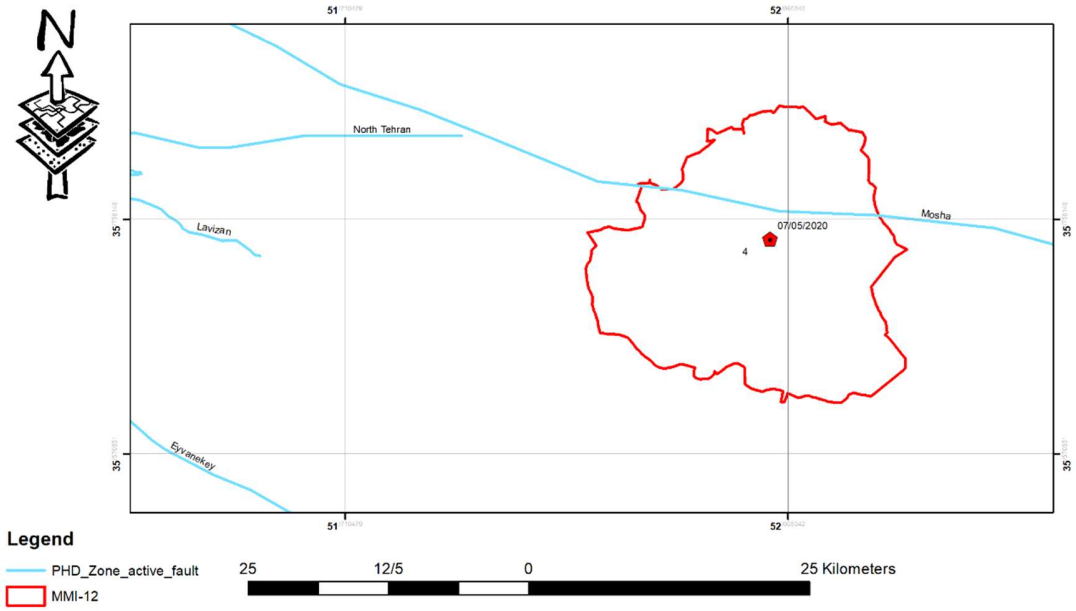

Figure 9. Definite zone Seismic sourcesmodel and zone isointensity (MMI) of magnitude 4 for the Damavand earthquake - 07/05/2020

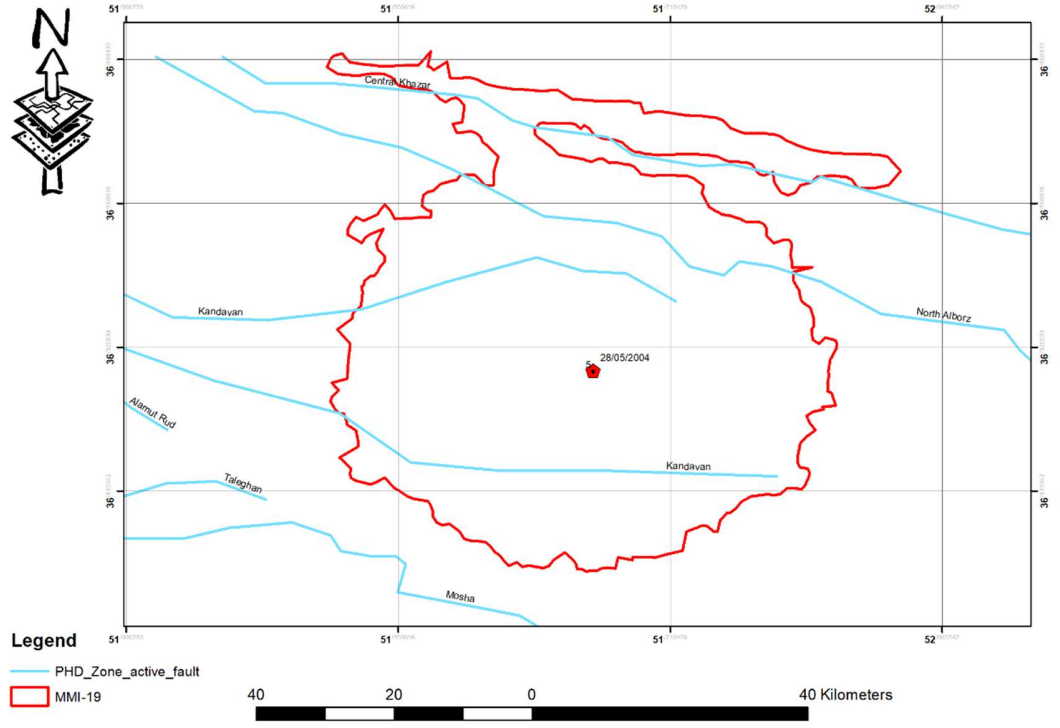

Figure 10. Deterministic model of zone Seismic sourcesand zone isointensity (MMI) of magnitude 5 for the Nowshahr earthquake - 28/05/2004

Seismic Absence "B": Identifying Potential Earthquake Seismic Sources in the Study Area

After determining the MMI and isointensity zones for the Garmsar earthquake on October 25, 1982, it appears that, due to the activity of the Garmsar fault, a 29.5 km segment of the eastern part of the Ivanki fault was locked. According to the "Zare (1374) (L = 37% LF)" relationship, this segment could potentially generate a maximum magnitude (MMax) of 5.8 on the Richter scale. However, part of this seismic gap was released during the 27 km-long segment of the Garmsar - earthquake on August 23, 1988, which had a magnitude of 5.2 Richter. Therefore, the study concludes that the eastern part of the Ivanki fault currently lacks the seismic potential for a future event and is unlikely to pose a significant hazard.

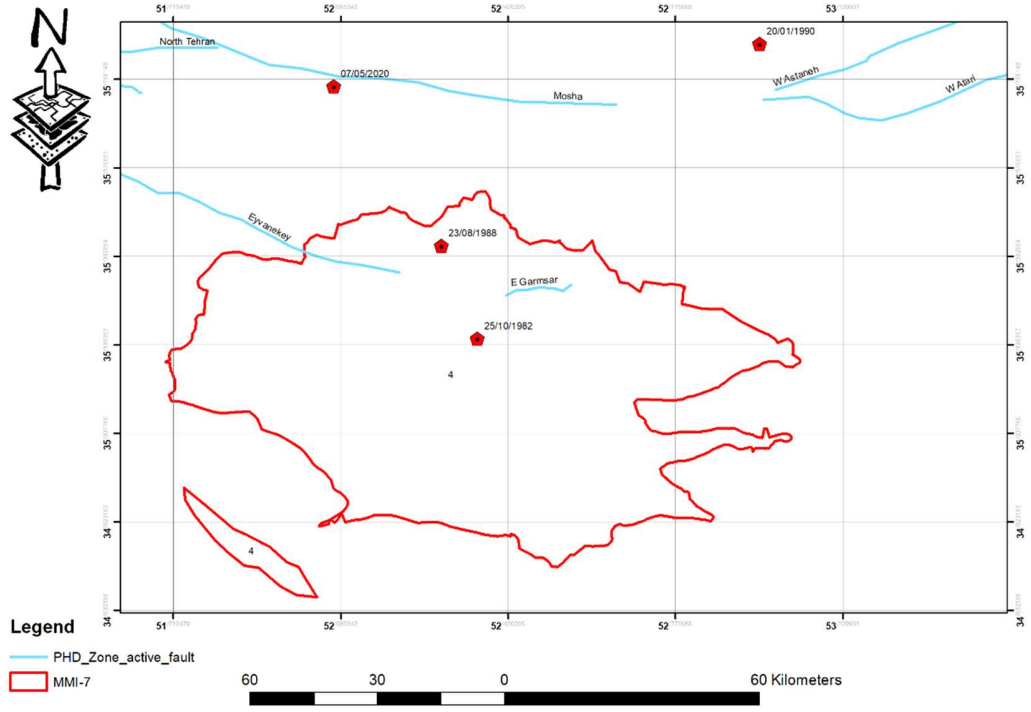

Figure 11. Definite model of zone Seismic sourcesand zone isointensity (MMI) of magnitude 4 for the Garmsar earthquake - 10/25/1982.

As shown in (Fig. 12) to (fig. 15), the deterministic models display the isoseismal zones (MMI) for significant events, including the 1957 Babol earthquake with a magnitude of 5 (Fig. 13), the 2017 Mallard earthquake with magnitude of 4 (Fig. 15), and the 2025 Javadabad earthquakes (magnitudes 3.3 and 3.0), which are mapped within the MMI zone of the 1982 Garmsar event (Fig. 14).

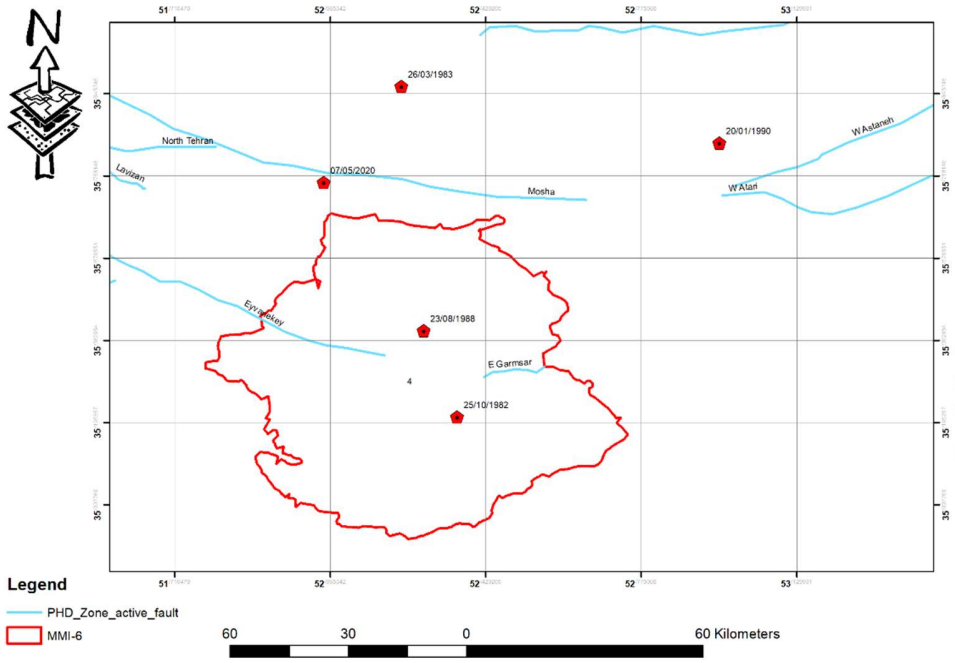

Figure 12. Definite zone Seismic sourcesmodel and zone isointensity (MMI) of magnitude 4 for the Garmsar earthquake - 23/08/1988

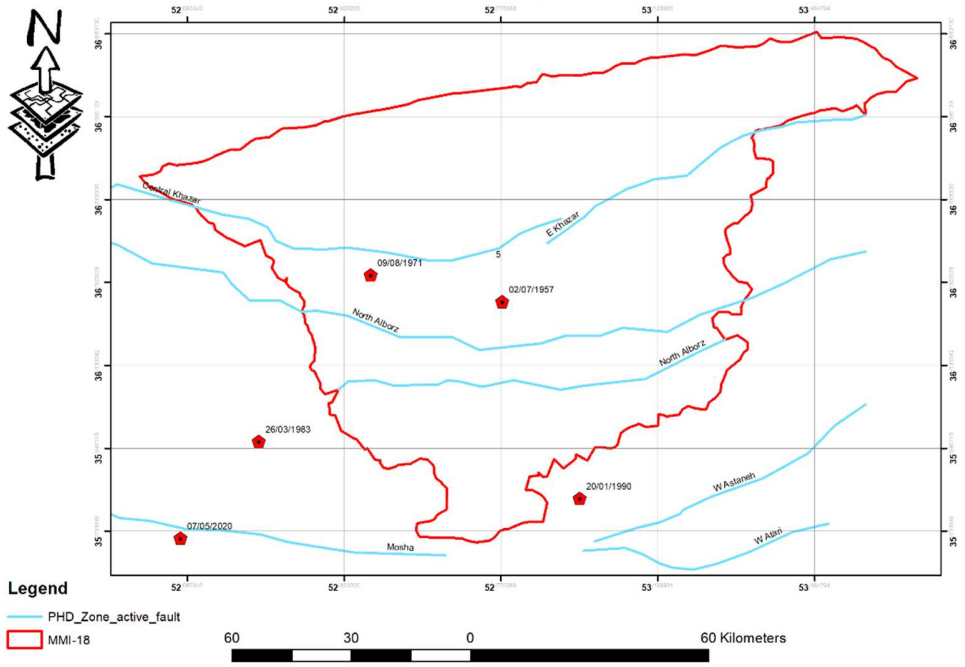

Figure 13. Deterministic model of the area Seismic sourcesand the area of isointensity (MMI) of magnitude 5 for the Babol earthquake - 02/07/1957

Validation of section "B" ,Two earthquakes with magnitudes of 3.3 and 3.0 on the Richter scale occurred on 24/12/1403 in Javadabad, Tehran, in the eastern part of the Ivanaki fault. According to the results of this study, the historical records and these micro-earthquakes likely do not indicate sufficient seismic potential for a major event in the short term and are therefore unlikely to pose a significant danger.

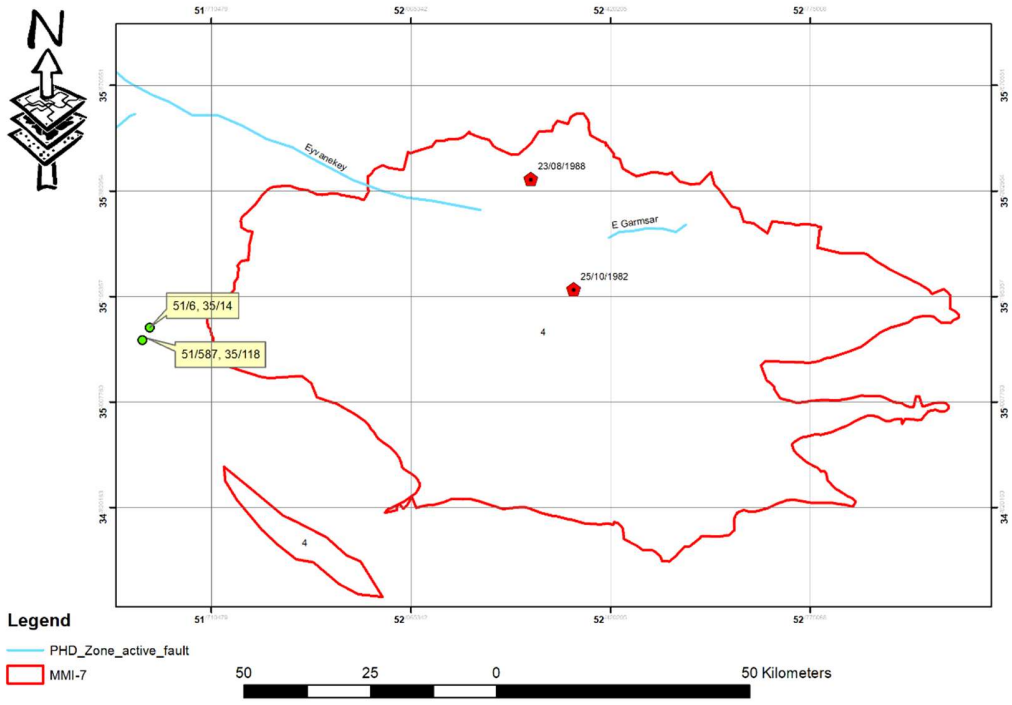

Figure 14. Location of the 3.3 and 3.0 Richter earthquakes of 24/12/1403 Javadabad, Tehran (green circles with coordinates on the left side of the image) in the deterministic zone Seismic sourcesmodel and zone of equal intensity (MMI) of 4 for the Garmsar earthquake - 25/10/1982 with a magnitude of 5.2 Richter

Seismic absence "C": To determine potential earthquake Seismic sourcesin the study area

After determining the MMI and isointensity zones for the Mallard seismic event on 12/20/2017, it appears that due to activity in the eastern part of the Eshtehard fault, an area 22.5 km long along the western segment of the North Tehran fault, an area 4 km long along the western segment of the Kahrizak fault, and a 2.5 km wide by 5 km long area of the Chitgar rupture zone have been locked. According to the "Zare (1374) (L = 37% LF)" relationship, a magnitude (MMax) of 5.6 on the Richter scale can be assumed for the western part of the North Tehran fault, and a magnitude of MMax=5.8 on the Richter scale for the Chitgar rupture zone. While part of this seismic

quiescence occurred in the 15 km long segment of the Tehran earthquake on 12/26/2017, which had a magnitude of 4.0, it can be concluded that a significant portion of the western North Tehran fault and the Chitgar rupture zone remain essentially unstressed and are likely candidates for introduction as faults capable of generating earthquakes in the near future. Furthermore, it can be inferred that the second earthquake, in addition to activating the aforementioned faults, induced microseismic activity along Tehran faults including Kaj Boulevard, Kon, Tarsht, and Bagh-e-Fayz. As shown in (Fig. 15) to (fig. 19), deterministic models illustrate the isoseismal zones (MMI) for several significant earthquakes: the 2017 Mallard earthquake magnitude 4, (Fig. 15), the 2017 Tehran earthquake magnitude 3, (Fig. 16), the 1971 Babol earthquake magnitude 5, (Fig. 17), and the 1990 Sool-e-Ben earthquake magnitude 5, (Fig. 18). Additionally, (Fig. 19) Presents the overlap of critical areas defined by Japan's JICA classification with zones identified as seismically inactive based on MMI analysis.

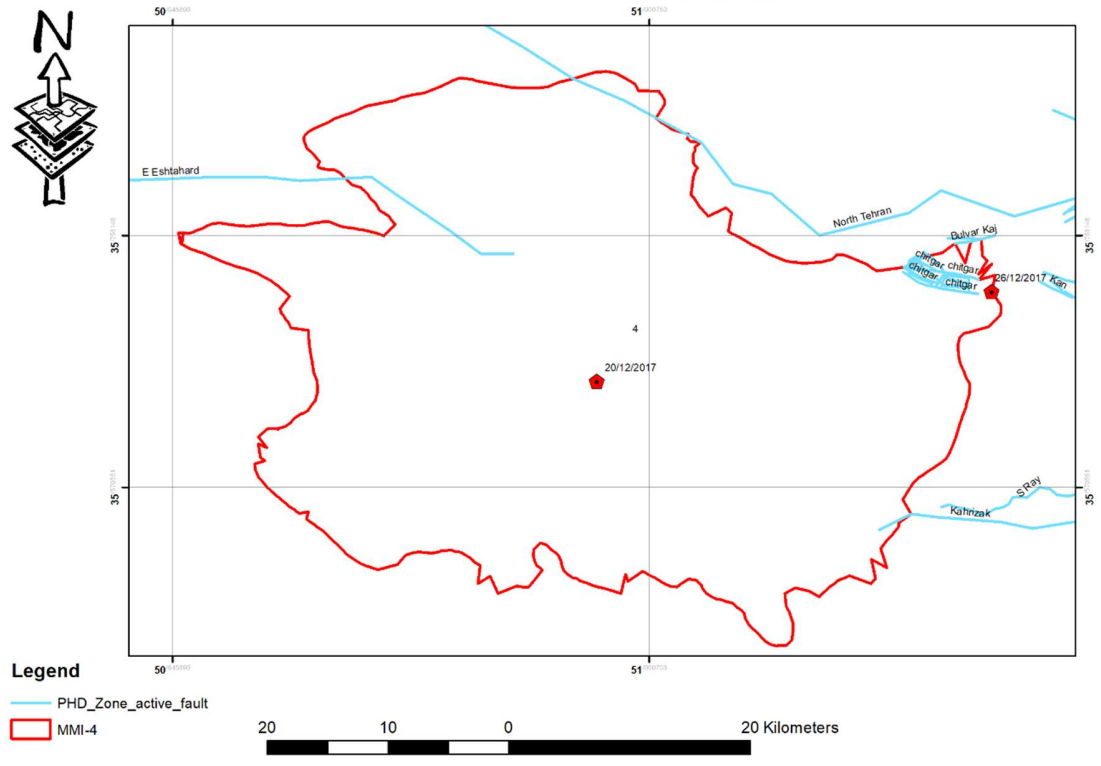

Figure 15. Definite zone Seismic sourcesmodel and zone isointensity (MMI) of magnitude 4 for the Mallard earthquake – 12/20/2017

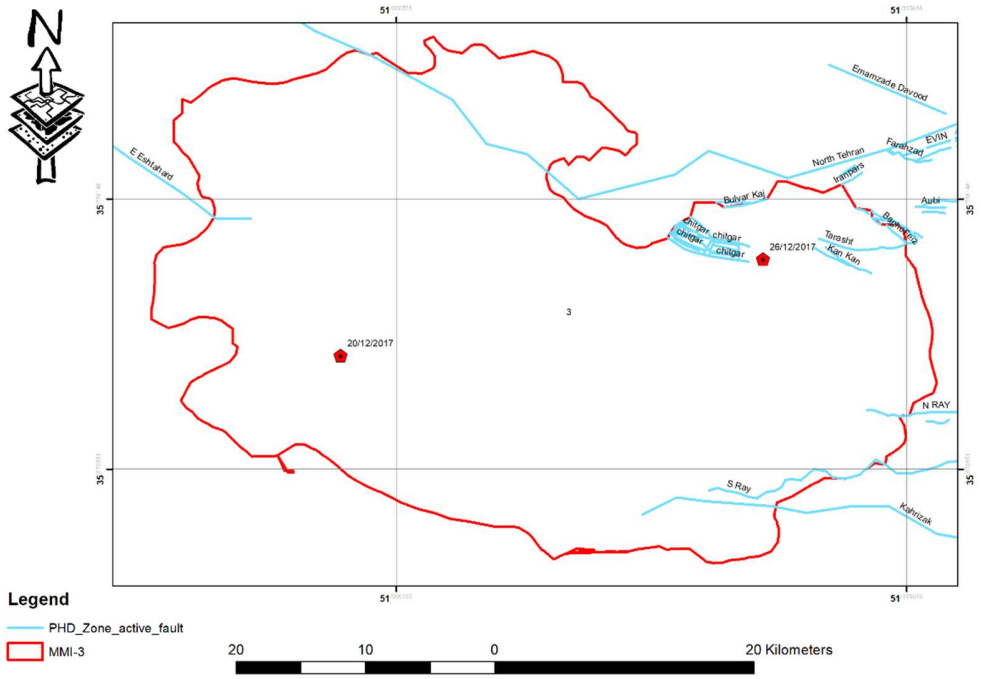

Figure 16. Deterministic model of zone Seismic sourcesand zone isointensity (MMI) of magnitude 3 for the Tehran earthquake – 12/26/2017

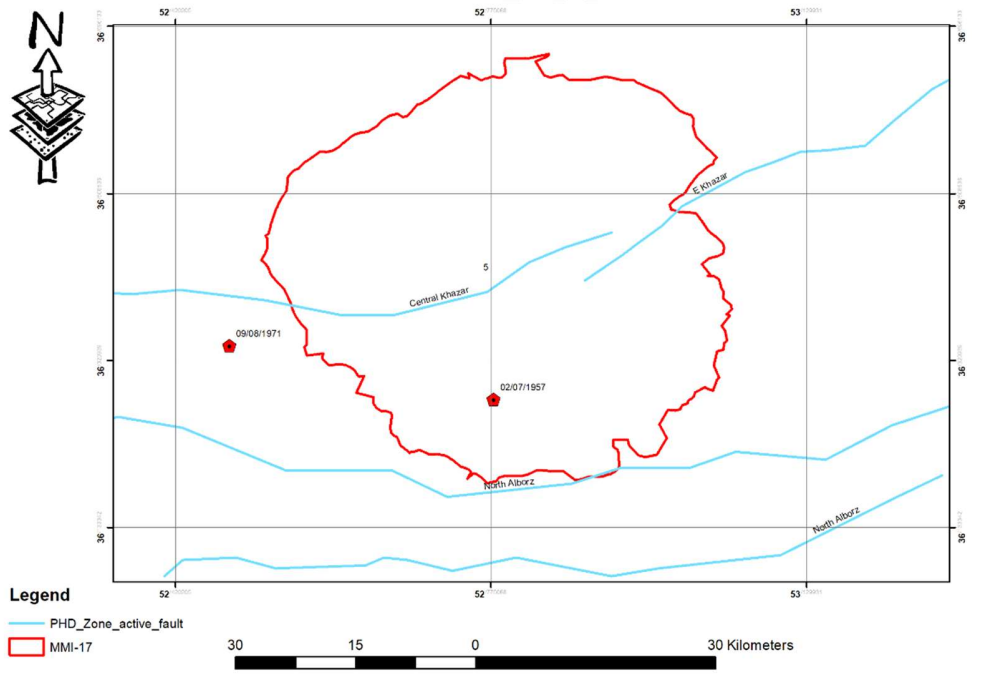

Figure 17. Deterministic model of zone Seismic sourcesand zone isointensity (MMI) of magnitude 5 for the Babol earthquake - 09/08/1971

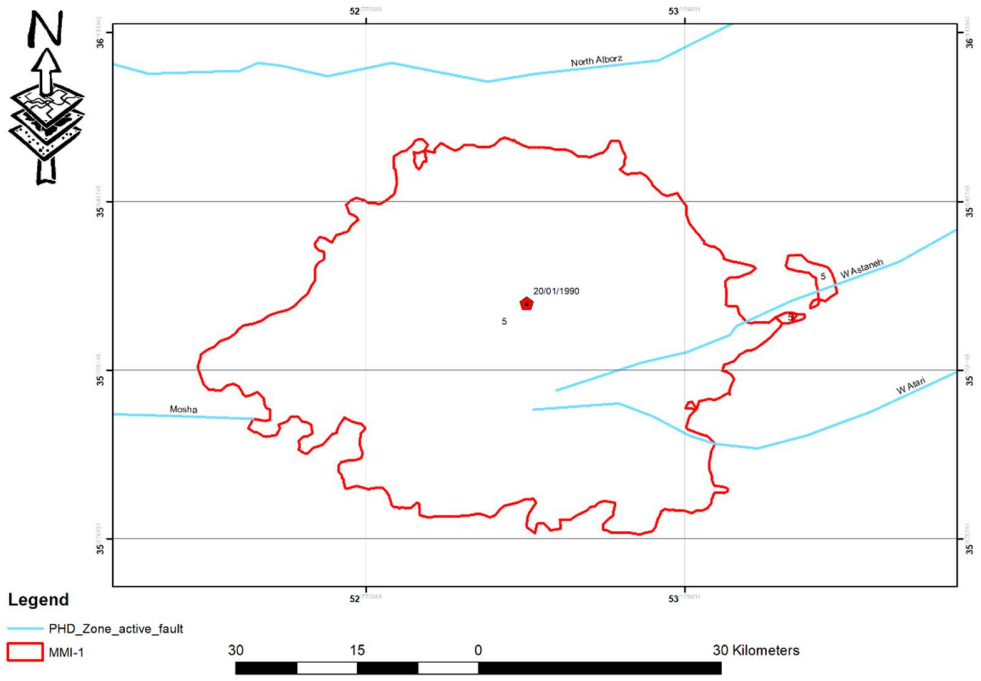

Figure 18. Deterministic model of zone Seismic sourcesand zone isointensity (MMI) of magnitude 5 for the Sool-e-Ben earthquake - 20/01/1990

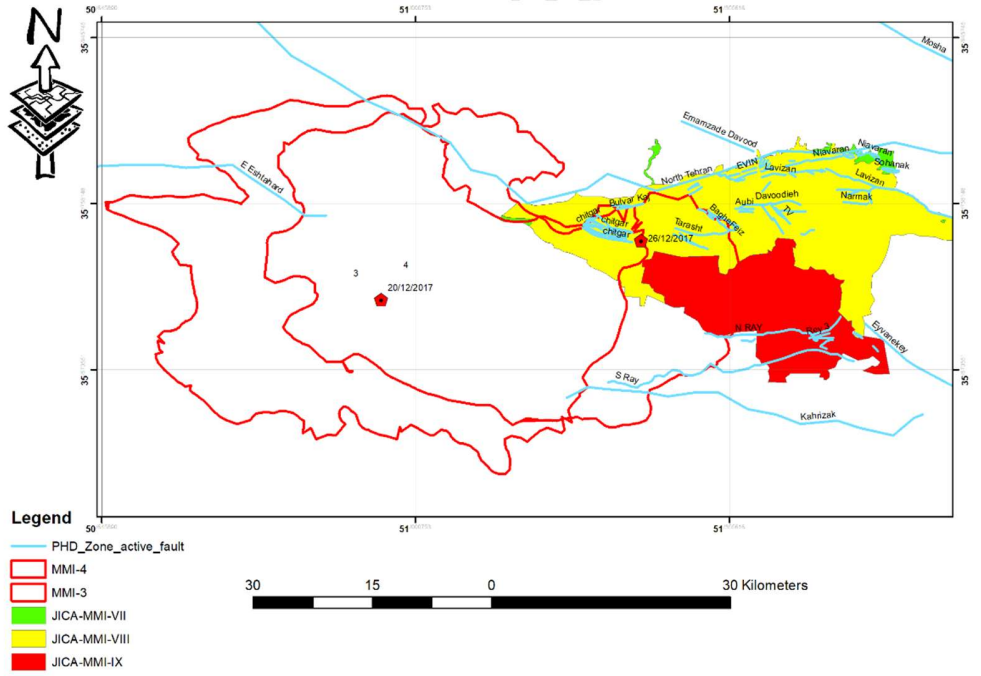

Figure 19. Overlap of critical areas designated according to Japan's JICA classification with areas designated as areas attributed to seismic absence based on MMI

6. Proposed deterministic model - Earthquake hazard estimation by summarizing the deterministic method

According to the survey conducted in the study area and the estimation of earthquake hazard using the deterministic method, the combined approach is referred to as the "deterministic model. model represents zonal seismic sources based on the visualization of the intersections of fault zones within the study area, taking into account the influence of hidden faults. It is grounded on the principle of future event buoyancy, which is attributed to the absence of seismicity in rupture areas surrounded by the main faults. The assumptions of the model are as follows (Fig. 20) and presented in the table 16:

- The study area was divided into four east-west bands, with band 1 representing the north and band 4 representing the south.
- Each band is considered as a potential zonal or volumetric earthquake Seismic sources(as the first step of the deterministic method). Since faults in this volume spring can interact, and in this case the entire length of the fault ruptures, we consider the average of their smallest magnitudes as the minimum possible magnitude for the volume spring.
- The largest historical event attributed to the components of the volume spring
- The maximum possible acceleration of the volume spring represents the largest possible computational acceleration in each region.
- The minimum possible acceleration of the volume spring represents the smallest possible computational acceleration in each region.
- The initial priority of the future event is determined using all the previous parameters and determines which: the first 5, the second 4, the third 3, and the fourth 2, are the regions where the possible future event will occur.
- Population (residential, schools, conference, etc.) and urban (building, road, workshop, etc.) texture is expressed numerically and shows the level of vulnerability in a possible future event in each volumetric Seismic sources (the highest vulnerability level is 5 and the lowest vulnerability level is 2).

- The final priority of the future event is the product of the initial priority value of the future event by the value of the population and urban texture, whose numerical range is from 4 (it has the lowest priority but does not mean no event!) to 25 (it has the highest priority and the possible future event will occur there and is extremely dangerous and damaging).

Table 16. Proposed four-zone deterministic model

Order of the area from top to bottom	Faults in the area Minimum probable	magnitude of the volumetric spring	Largest attributable historical event	Maximum probable acceleration g(cm/s2)	Minimum probable acceleration g(cm/s2)	Initial priority of the future event	Population and urban texture	Final priority of the future event
1	Mosha and North Tehran, Taleghan and Kandovan	6.9	7.7	815	448	5	2	C = 10
2	Niavaran and Eshtehard	6	7.2	448	315	2	3	D = 6
3	North Rey and Robat Karim	6.1	7.7	520	300	4	5	A = 20
4	Ivanaki and Kahrizak and South Rey and Pieshva	6	7.7	495	315	3	4	B = 12

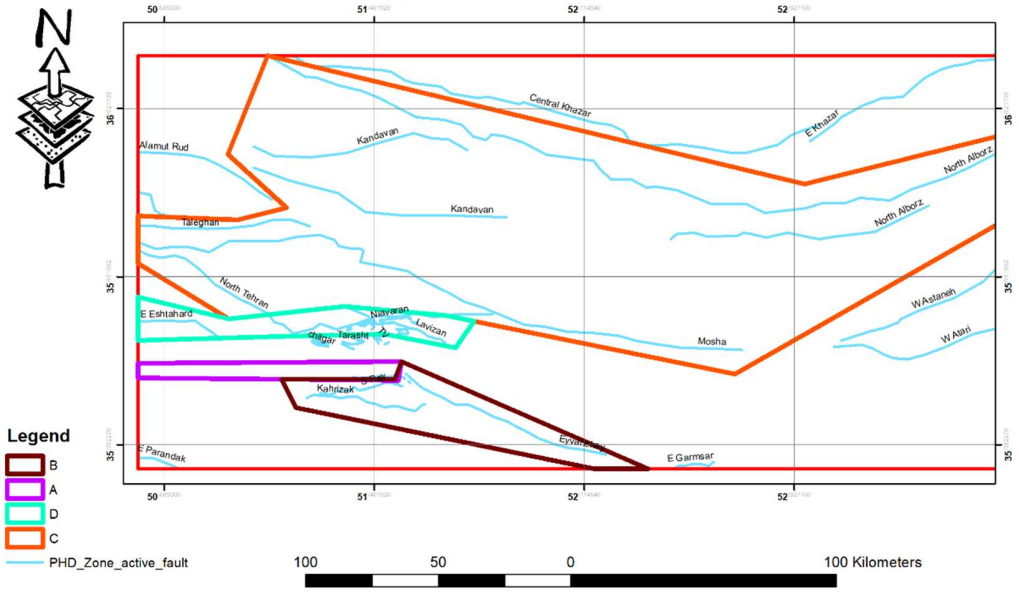

Figure 20. Placement of the four-zone deterministic model in the study area

** Note: Priorities "A, B, C, D" are the first to fourth possible future events in the study area, respectively.

6.1. Investigating the potential social and economic impacts of future earthquakes in the study area

Potential Socio-Economic Impacts of Future Earthquakes in Tehran and Central Alborz:Large earthquakes can have widespread impacts on the social and economic structure of urban areas. Tehran and Central Alborz are at serious risk due to their high population density, sensitive infrastructure, and active tectonic location (Zareian, 2023).Social impacts of future earthquakes: Increased social vulnerability, reduced social cohesion in affected areas, especially in underserved neighborhoods, increased internal migration due to the destruction of residential areas and reduced quality of life, increased unemployment due to business closures and reduced job opportunities Crisis management and social response: Lack of relief resources and challenges in distributing first aid, increased pressure on health systems due to the high number of injured and the need for medical services, psychological and social impacts such as anxiety, depression, and reduced public trust (Zareian, 2023)Economic impacts of future earthquakes: Destruction of urban infrastructure and reconstruction costs, damage to critical buildings and facilities such as hospitals, schools, and transportation networks, increased reconstruction costs that may take years, decreased real estate values in affected areas (Bacbronowicz, 2024)

Impact on regional and national economies: Disruption of economic activities due to the destruction of commercial and industrial centers, decreased gross domestic product (GDP) due to reduced productivity and increased reconstruction costs, Increase in inflation rate due to increased demand for essential goods and servicesStrategies to reduce the socio-economic impacts of earthquakes: Improving urban resilience programs to reduce infrastructure damage, increasing social preparedness and public education for crisis management, creating financial funds and earthquake insurance to reduce economic pressure on citizensAccording to the above, a future earthquake in Tehran and the central Alborz could have widespread impacts on the social and economic structure of these regions. Crisis management, infrastructure resilience, and increasing social preparedness can help reduce these impacts (Zare et al., 2020).

6.2. Investigating the potential impacts of future earthquakes in Tehran and Central Alborz:

Large earthquakes in Tehran and Central Alborz, especially in sensitive areas such as the Shomal-Rey Fault and the Robat-Karim Fault, could have widespread impacts on critical infrastructure,

economic costs, and mitigation strategies. These areas are at serious risk due to their high population density, presence of critical facilities, and active tectonic location (Ziari et al., 2025).

Potential impacts on critical infrastructure:

a) Transportation and communication networks,Road and bridge damage: Large earthquakes can cause bridges to collapse, roads to crack, and major routes to be blocked, making relief efforts difficult.Damage to telecommunication networks: Interruption of emergency communications can disrupt coordination of relief and rescue operations.Disruption to public transport: Metros, buses and railways may suffer structural damage, reducing people's access to essential services.

b) Energy and water facilities,Damage to power plants and transmission lines: Earthquakes can cause widespread power outages, which can have severe impacts on hospitals, relief centres and industrial facilities, Disruption to water and sewage networks: Broken water and sewage pipes can cause health crises and spread water-related diseases.Damage to gas facilities: Gas leaks caused by earthquakes can increase the risk of fires and explosions, Economic costs of earthquakes:

c) Direct and indirect costs (Iura, 2024), Costs of rebuilding infrastructure: The destruction of buildings, bridges and critical infrastructure can cost billions of dollars.Decrease in Gross Domestic Product (GDP): Business closures and reduced productivity can affect regional and national economies.Increased insurance and investment costs: Increased seismic risk will increase insurance rates and reduce investment in affected areas.

d) Impact on the real estate market and investment, Decrease in property values in affected areas: Large earthquakes can cause economic recession in the real estate sector.Increased reconstruction and retrofitting costs: Owners and the government must make large investments in reconstruction and retrofitting.Strategies to reduce the effects of earthquakes:

e) Resilience of critical infrastructure, Improving structural design: Using modern resilience technologies to increase the resistance of buildings to earthquakes, Upgrading early warning systems: Developing early warning systems to reduce human and economic losses, Strengthening transportation and communication networks: Resilience of bridges, roads, and telecommunication networks to reduce potential damage

f) Crisis management and social preparedness, Rapid response planning: Creating crisis management plans to increase relief capacity, Public education and raising public awareness: Holding training courses and earthquake drills to reduce social damage, Establishing financial funds and earthquake insurance: Providing financial resources to help rebuild and support the

affected, Accordingly, a future earthquake in Tehran and the central Alborz could have widespread impacts on critical infrastructure, the economy, and society. Infrastructure resilience, improved crisis management, and increased social preparedness can help mitigate these impacts.

7. Conclusion

This paper presents a seismic gap analysis of the Tehran and Central Alborz regions by integrating Modified Mercalli Intensity (MMI) and Peak Ground Acceleration (PGA) data with fault geometry and historical earthquake catalogs. Employing a deterministic, GIS-based approach, the study identifies zones of seismic locking and prioritizes them for potential future earthquakes, resulting in a four-zone hazard model that highlights areas of greatest vulnerability.

A model has been developed using the modified Mercalli isointensity zones, magnitude, intensity, and the relationships between the seismic event's energy, magnitude, and ground motion forces. This model aims to estimate the initial future event attributed to the absence of seismicity in the study area, yielding the following results:

The findings of this study underscore critical concerns regarding seismic hazards in the Tehran region. Notably, the most prominent seismic gaps identified in the analysis are attributed to previously unknown faults within the Tehran area, highlighting the urgent need for intensified monitoring and investigation of these fault segments. Given the presence of a fault approximately 20 kilometers in length with a displacement of 50 centimeters per seismic event, it is estimated that such a structure could generate earthquakes with magnitudes up to 6.5 on the Richter scale, potentially leading to highly destructive outcomes.

Deterministic modeling results indicate that the southeastern region of Tehran Province has a high potential for seismic activity. Among the major fault systems, the North Rey Fault and the Robat-Karim Fault are of particular concern, as both are capable of generating seismic events with magnitudes of 7 or greater. Based on the analytical parameter "Ultimate Priority of Future Event," the urban areas affected by these faults are identified as the most vulnerable zones in the event of a future earthquake in Tehran.

Subsequent priority levels are assigned to other fault systems in the following order: (1) Ivanaki and Kahrizak faults, along with the South Rey and Pishva faults; (2) Mosha and North Tehran faults, along with the Taleghan and Kandovan faults; and (3) Niavaran and Eshtehard faults.

Although the Mosha Fault has potential for seismic activity in the central and western parts of the region, it is considered to have relatively low priority for future seismic events based on the results

of this study. Furthermore, changes in the VS30 shear wave velocity are used to determine the discontinuity boundaries, fault characteristics, and soil types at the construction site. The length of the involved fault and variations in wave velocity serve as auxiliary factors in identifying areas likely to be seismically inactive.

Determining the development of vulnerability and its impact from seismic site effects is closely related to the progression of strong ground motion and the most probable scenarios for damage resulting from future earthquakes in vulnerable areas. Therefore, the most important population centers in the region are identified based on the classification of seismic site effects and their location relative to fault segments, using the parameter "vulnerability intensity in a future event, shown in Table 15, the classification of seismic site conditions (SSC) and the corresponding levels of vulnerability severity for each fault segment within the study area have been systematically evaluated.

This classification offers a comprehensive overview of the anticipated site response characteristics and their potential impact on seismic hazards during future events. By correlating geological, geotechnical, and seismological parameters, the table identifies fault segments with a higher susceptibility to amplification effects, indicating increased vulnerability. These insights are essential for prioritizing mitigation efforts, guiding land-use planning, and informing seismic risk assessments in the region. Presented in the table 17.

Table 17. Classification of SSC seismic site effect and severity of vulnerability in future events for segments or faults in the study area

Segment/Fault	Seismic Site Impact Classification SSC	Severity of vulnerability in future event	Segment/Fault	Seismic Site Impact Classification SSC	Severity of vulnerability in future event
Velanjak	Yellow (Very Dense Soil and Rock)	Medium	Kaj Boulevard	Yellow (Very Dense Soil and Rock)	Low
Tarsht	Yellow (Very Dense Soil and Rock)	Low	Beheshti University	Yellow (Very Dense Soil and Rock)	Moderate
Tonbakui	Yellow (Very Dense Soil and Rock)	Low	Fayz Garden	Yellow (Very Dense Soil and Rock)	Low
Southern Ray	Yellow + Pale Green (Hardened Soil)	High	Abbas Abad	Yellow (Very Dense Soil and Rock)	Low
Sohank	Yellow (Very Dense Soil and Rock)	Medium	Television	Yellow (Very Dense Soil and Rock)	Moderate
Buali Town	Yellow (Very Dense Soil and Rock)	Medium	Vank Park	Yellow (Very Dense Soil and Rock)	Moderate
Narmak	Yellow (Very Dense Soil and Rock)	Low	Davoodieh	Yellow (Very Dense Soil and Rock)	Low
Northern Ray	Pale Green (Hardened Soil)	High	TakhtTavous	Yellow (Very Dense Soil and Rock)	High

Northern Jantabad	Yellow (Very Dense Soil and Rock)	Medium	Niavaran	Yellow + Pale Green (Hardened Soil)	High
Farahzad	Yellow (Very Dense Soil and Rock)	Medium	Lavizan	Yellow + Pale Green (Hardened Soil)	Severity of vulnerability in future event
Avin	Yellow (Very Dense Soil and Rock)	Low	Inqlab	Yellow (Very Dense Soil and Rock)	Low
Chitgar	Yellow + Pale Green (Hardened Soil)	High			

By overlaying the seismic site effect zones with the strong ground motion zoning map based on Iran's Regulation 2800 (Design of Buildings Against Earthquakes), it was found that the faults within the study area predominantly coincide with zones characterized by Vs30 shear wave velocities ranging from 180 to 360 m/s. These zones, typically represented in light green, correspond to hardened soil types. Consequently, they indicate areas where seismic stress amplification is more likely to occur, increasing the potential for structural damage during future seismic events. Additionally, the most accurate linear Gutenberg-Richter relationship for the study area was derived using data from the IIEES, IRSC, and USGS seismic catalogs. This relationship provides a reliable basis for future seismic hazard assessments and modeling efforts in the region.

References

Xu R., Wang L. (2021) The horizontal to vertical spectral ratio andits applications, *EURASIP Journal on Advances in Signal Processing*, 2021:75, *Springer Open*. DOI: https://doi.org/10.1186/s13634-021-00765-z

Maghami S. H., Sohrabi-Bidar A., Bignardi S., Zarean A., Kamalian M. (2021) Extracting the shear wave velocity structure of deep alluviums of "Qom" Basin (Iran) employing HVSR inversion of microtremor recordings; *Journal of Applied Geophysics* 185 104246. DOI: https://doi.org/10.1016/j.jappgeo.2020.104246

MunaffNaji D., Akin M. K., FiratCabalar A. (2020) A Comparative Study on the VS30 and N30 Based Seismic Site Classification in Kahramanmaras, Turkey, *Hindawi Advances in Civil Enginering* . DOI: https://doi.org/10.1155/2020/8862827

IsmetKanl A., Tildy P., onay Z., Pınar A., Hermann L. (2006) VS30 mapping and soil classification for seismic site effect evaluation in Dinar region, SW Turkey, *Geophysics. J. Int*. ,165, 223–235._DOI: https://doi: 10.1111/j.1365-246X.2006.02882.x

Aung A.M.W., Leong E.C. (2015) Application of weighted average velocity (WAVe) method to determine Vs30, *The Japanese Geotechnical Society, Soils and Foundations*, 55(3):548–558. DOI: https://doi.org/10.1016/j.sandf.2015.04.007

Zare M., Bard P., Ghaforyashtiany M. (1999) Site characterizations from the Iranian strong motion network. *Cancer Research* ,71(89), 74–94. DOI: https://doi.org/10.1016/S0267-7261(98)00040-2

Lee C. T., Cheng C. T., Liao C. W., Tsai, Y. B. (2001) Site classification of Taiwan free field strong motion stations, *Bulletin of the Seismological Society of America*, *91*(5), 1283-1297. DOI: https://doi.org/10.1785/0120000736

Anbazhagan P., Srilakshmi K.N., Bajaj K. (2019) Determination of seismic site classification of seismic recording stations inthe Himalayan region using HVSR method, *Soil Dynamic and Earthquake Engineering*, 116, 304–316. DOI: https://doi.org/10.1016/j.soildyn.2018.10.23

Malhotra P. K. (2021) Seismic Analysis of Structures and Equipment, *Chapter 2: Ground Motions for Future Earthquakes, Springer.* DOI: https://doi.org/10.1007/978-3-030-57858-9_2

Douglas J. (2003) Earthquake Ground Motion Estimation Using Strong Motion Records: A Review of Equations for the Estimation of Peak Ground Acceleration and Response Spectral Ordinates, *Earth Science Reviews.* DOI: https://doi.org/10.1016/S0012-8252(02)00112-5.ISSN

Zare M. (2017) Seismic Hazard Zoning in Iran: A State of the Art on the Studies during Four Decades, *JSEE*, Vol. 19, No. 2.

Aram M. R., Hassankhani A. (2017) Simulation of Strong Ground Motion and Development of Attenuation Relationships for the Bushehr Nuclear Power Plant Site Based on the Stochastic Finite Fault Method, *Journal of Nuclear Science and Technology*, 81, 58-72. DOI: https://dor.isc.ac/dor/20.1001.1.17351871.1396.38.3.7.9

Zaferani H., Noorzad A. (2013) Earthquake engineering and earthquake simulation, *Tehran University Press*.

GhodratiAmiri G. H. R., RezvianAmrei S. A. L., RezvianAmrei S. A. M. (2018) Development of Acceleration Attenuation Relationships for the Iranian Plateau, *Journal of Modeling in Engineering*, Volume 16, Issue 54. DOI: https://doi.org/10.22075/jme.2017.4629

GhodratiAmiri G. (2007) Attenuation Relationships for Iran, *Journal of Earthquake Engineering*, 11:4, 469-492. DOI: https://doi:10.1080/13632460601034049

Zare M. (2017) Recent development of the earthquake strong motion intensity catalog and intensity prediction equations for Iran, *J Seismol* 21, 591–613. DOI: https://doi.org/10.1007/s10950-016-9622-4

Bulut F., Özener H., Doğru A., Aktuğ B., Yaltırak C. (2018) Structural setting along the Western North Anatolian Fault and its influence on the 2014 North Aegean Earthquake (Mw 6.9), Volume 745, 16 October 2018, Pages 382-394. DOI: https://doi.org/10.1016/j.tecto.2018.07.006

Tavakoli B., Ghaforyashtiany M. (1999) Seismic hazard assessment of Iran, *Annals of Geophysics*, *42*(6). DOI: https://doi.org/10.4401/ag-3781

Rashidi A., Nemati M., Shafieibafti S. H., Pourbeyranvand S. H., Derakhshani R., Braitenberg C. (2023) Structure and kinematics of active faulting in the northern domain of Western and Central Alborz, Iran and interpretation in terms of tectonic evolution of the region, *Journal of Asian Earth Sciences*, Volume 255, 105760. DOI: https://doi.org/10.1016/j.jseaes.2023.105760

Mohammadi Nia A., Rashidi A., Khatib M. M., Mousavi S. M., Nemati M., Shafieibafti S., Derakhshani R. (2023) Seismic Risk in Alborz: Insights from Geological Moment Rate Estimation and Fault Activity Analysis, *Applied Sciences*, *13*(10), 6236. DOI: https://doi.org/10.3390/app13106236

Tourani M., Isik V., Saber R. et al. (2024) Evaluation of seismicity and seismotectonics in the Alborz Mountains: insights from seismic parameters, *Northern Iran. J Seismol* 28, 675–706. DOI: https://doi.org/10.1007/s10950-024-10218-3

Bastami M., Kowsari M. (2014) Seismicity and seismic hazard assessment for greater Tehran region using Gumbel first asymptotic distribution, *Structural Engineering and Mechanics,* Vol. 49, No. 3, 355-372. DOI: https://doi.org/10.12989/sem.2014.49.3.355

Alikhanzadeh R., Zafarani H. (2023) Physics based probabilistic seismic hazard analysis: the case of Tehran Basin in Iran. *Bull Earthquake Eng*, 21, 6171–6214. DOI: https://doi.org/10.1007/s10518-023-01785-w

Boostan E., Tahernia N., Shafiee A. (2015) Fuzzy probabilistic seismic hazard assessment, case study: Tehran region, Iran, *Natural Hazards*. DOI: https://doi:10.1007/s11069-014-1537-1

Motaghed S., Khazaee M., Eftekhari N., Mohammadi M. (2023) A non extensive approach to probabilistic seismic hazard analysis, *Nat Hazards Earthe*, 23, 1117–1124. DOI: https://doi.org/10.5194/nhess-23-1117-2023

Zareian M. (2023) Social capitals and earthquake: A Study of different districts of Tehran, Iran, Vol. 5 No. 2: *International Journal of Disaster Risk Management (IJDRM)*. DOI: https://doi.org/10.18485/ijdrm.2023.5.2.2

BacBronowicz J. (2024) Mapping Social Vulnerability to Earthquake Hazards by using Analytic Hierarchy Process (AHP) and GIS in Tehran City, *Institute of Geodesy and Geoinformatics*, 152-52 Sugo,*Takizawa, Iwate, Japan*.

Zare M., Memarian H., Kamranzad F. (2020) Earthquake Risk Assessment for Tehran, *Iran, ISPRS Int. J. Geo-Inf.* DOI: https://doi.org/10.3390/ijgi9070430

Iura A. (2024) Economic and financial elements of critical infrastructure augmentation, *International Conference knowledge based organization.* DOI: https://doi.org/10.2478/kbo-2024-0051

Ziari K., Zare S. H., Abbas R. A. (2025) The challenges of sustainability in urban planning (the metropolis of Tehran), *Journal of Infrastructure*, 9(2), 10085. DOI: https://doi.org/10.24294/jipd10085

Bommer J.J., Verdon J.P. (2024) The maximum magnitude of natural and induced earthquakes Geomech. *Geophys. Geo-energ*., 10, 172. DOI: https://doi.org/10.1007/s40948-024-00895-2

Rivasmedina A., Benito B. (2018) and Jorge Miguel Gaspar Escribano, Approach for combining fault and area sources in seismic hazard assessment: application in south-eastern Spain, *Nat. Hazards Earth Syst. Sci*., 18, 2809–2823. DOI: https://doi.org/10.5194/nhess-18-2809-2018

Vats F., Basu D. (2023) On the construction of Joynerboore distance (Rjb) for PESMOS and COSMOS databases, *J Seismol* ,27, 173–202. DOI: https://doi.org/10.1007/s10950-022-10129-1

Bommer J. J., Akkar S. (2012) Consistent Source-to-Site Distance Metrics in Ground Motion Prediction Equations and Seismic Source Models for PSHA, *Earthquake Spectra, Volume* 28, No. 1, pages 1–15, Earthquake Engineering Research Institute. DOI: https://doi.org/10.1193/1.3672994

Gupta I.D. (2013) Source to site distance distributions for area type of seismic sources used in PSHA applications. *Nat Hazards* 66, 485–499. DOI: https://doi.org/10.1007/s11069-012-0498-5

Pourmohammad F., Zare M. (2023) earthquake hazard analysis in alborz provice IRAN, *Canadian Conference Pacific Conference on Earthquake Engineering 2023 Vancouver, British Columbia*.

Taroni M. (2023) Estimating the Magnitude of Completeness of Earthquake Catalogs Using a Simple Random Variable Transformation, *The Seismic Record.* DOI: https://doi: 10.1785/0320230017

Karaca H. (2024) Hazard functions and conditional probability of earthquake occurrences in major fault zones in Turkey, *Iranian Journal of Earth Sciences*, *15*(2). DOI: https://doi.org/10.30495/ijes.2022.1952666.1722

Yazarloo R., Khamehchiyan M., Nikudel M. R. (2021) Geological and engineering geological characteristics of surface alluviums in the Gorgan city, *Iranian Journal of Earth Sciences*, *14*(2), 141-149. DOI: https://doi.org/10.30495/ijes.2022.690880

Norouzi, Mohajerashai (1978) Relationship between fault length and magnitude of earthquake hazard.

Ritz J. F., Nazari H., Balescu S., Lamothe M., Salamati R., Ghassemi A., Shafei A., Ghorashi M., Saidi A., (2012) Paleoearthquakes of the past 30.000 Years along the North Tehran Fault (Iran), *Journal of Geoohysical Research*, Vol. 117, B06305. DOI: https://doi.org/10.1029/2012JB009147

Wells D.L., Coppersmith K.J. (1994) New Empirical Relationships Among Magnitude, Rupture Length, Rupture With, Rupture Area and Surface Displacement, *Bulletin of the Seismological Society of America*, Vol. 84, No. 4, PP 974-1002.

Aghanabati A. (2004) The Geology of Iran. *Geological Survey of Iran*, *Tehran*, 586 p.

Tchalenko J.S. (1974) Outline of Seismotectonic Provinces of North Central Iran, In Materials for the Study of Seismotectonics of Iran. DOI: https://doi.org/10.1016/B978-0-444-41420-5.50050-2

Tchalenko J.S. (1974) Recent Destructive Earthquake in the Central Alborz, In Materials for the Study of Seismotectonics of Iran. DOI: https://doi.org/10.1016/0040-1951(75)90169-9

Tchalenko J.S., Berberian M., Iranmanesh H., Bailly M., Arsovsky M. (1974) Tectonic Framework of the Tehran Region.

Ambraseys N.N., Berberian M. (1976a) Historical Seismicity of North Central Iran in Materials for the Study of Seismotectonics of Iran, *Contribution to the Seismotectonic of Iran (part II), Report* No. 39, *Geological Survey of Iran,*

Berberian M. (1976b) Generalized Fault Map of Iran, Acale 1:5000000, Geological Survey of Iran.

Berberian M., Yeats R.S. (2001) Contribution of Archaeological data to Studies of Earthquake History in the Iranian Plateau, J. *Struct. Geol*., 23, 563-584.

Berberian M., Yeats R.S. (1999) Patterns of Hitorical Earthquake Rupture in the Iranian Plateau, *Bull. Seism. Soc. Am*., 89, 120-139. DOI: https:// doi.org/10.1785/BSSA0890010120